2026 SPE Improved Oil Recovery Conference

SPE 231509-MS

Testing an Improved Method to Determine Inaccessible Pore Volume

R.S. Seright[1]*

[1]Petroleum Recovery Research Center, New Mexico Tech, Socorro, NM, USA
*Corresponding author; randy.seright@nmt.edu

Abstract

Inaccessible pore volume (*IAPV*) is intended to characterize the fraction of aqueous pore space in a porous medium that is not accessible to flowing polymer. Previous *IAPV* literature is contradictory in that no correlation is evident between measured *IAPV* values and rock permeability or porosity or polymer molecular weight or size in solution. Prior work by Gilman and MacMillan (1987) and Wang et al. (2021) demonstrated that much of the previous contradictory reports may result from the inadequacies of methods to measure *IAPV*. In particular, the "double-polymer/tracer bank" method incorporates a water flush between two polymer/tracer banks. The unfavorable mobility ratio as water displaces the second polymer bank causes viscous fingering and overestimation of *IAPV* if insufficient water is flushed. Dean et al. (2022) proposed a potentially improved method to determine *IAPV*, where a low concentration polymer bank is displaced by a more-concentrated, more-viscous polymer bank—so the mobility ratio is always favorable during the displacement. This paper tests this method for determining *IAPV*.

The tests used sandstone cores and bead packs with permeabilities ranging from 113 to 18600 mD, porosities ranging from 0.188 to 0.402, and core lengths ranging from 30.48 to 122-cm. Many tests involved 500-ppm HPAM (with no potassium iodide tracer) displacing 250-ppm HPAM (with a KI tracer). However, three sets of tests made five replicate determinations of *IAPV* using successive polymer banks with HPAM concentrations starting at 62.5 ppm and doubling in stages to 2000 ppm. This procedure tested the reproducibility of the method and whether the *IAPV* measurement depended on HPAM concentration.

With a given data set, multiple methods can be used to assign an *IAPV* value, including (1) the area between polymer and tracer breakout curves, (2) the difference in pore volume (*PV*) throughput (between polymer and tracer) upon attaining an effluent concentration of 50% of the injected concentration, and (3) the difference in *PV* during first breakout of polymer ahead of tracer. Significant differences in calculated *IAPV* values were noted for these different methods.

In general, the method of Dean et al. (2022) provides a substantial improvement over previous methods when measuring *IAPV*. However, caution must be exercised when interpreting the results of these tests with respect to projecting polymer-flood performance. Important uncertainties arise from assessments of *IAPV*—notably, in rock with permeability above 200 mD. These uncertainties arise partly because polymer retention can vary with polymer concentration—violating a key assumption of the method of Dean et al. From this work, it is arguable whether a significant *IAPV* exists in Berea sandstone or bead packs with permeability greater than 200-mD (when using 18-20-million g/mol HPAM).

Introduction

In concept, inaccessible pore volume (*IAPV*) is the fraction of the aqueous-phase pore volume that cannot be accessed by large polymer molecules (Dawson and Lanz 1972). In addition to pores with very small entry points (pore throats), some (Chauveteau 1981; Sorbie 1991; Stavland et al. 2010; Akbari et al. 2019; Skauge et al. 2021; Dean et al. 2022) argued that *IAPV* could also include pore space close to a pore wall, because the radius of a large polymer molecule limits how close the center of mass for the molecule can approach the rock surface. However, Manichand and Seright (2014), Wang et al. (2021), and Seright and Wang (2023a) pointed out major flaws with these "depletion layer" arguments. *IAPV* has been advocated to accelerate polymer transit of a porous medium, while retention (e.g., adsorption onto the rock) retards it (Green and Willhite 1998). Thus, one might argue that *IAPV* facilitates oil displacement, although some have speculated that oil trapped in *IAPV* pores may no longer be available for displacement (Delamaide 2014. Akbari et al. 2019).

The double polymer/tracer method. The above conceptual arguments and definitions may need refinement in view of substantial limitations associated with existing methods of measuring *IAPV*. Although a number of methods have been used in the past (Dawson and Lantz 1972; Manichand and Seright 2014; Akbari et al 2019; Seright and Wang 2023a), the most accepted method to measure *IAPV* in the petroleum literature has been the "double-polymer/tracer-bank" method (Lotsch et al. 1985). Here (**Figure 1**), a bank containing both polymer (e.g., HPAM) and a water tracer (e.g., potassium iodide, KI) is injected into a porous medium that is saturated with water (containing no tracer). The effluent from the core is monitored for concentrations of both the polymer and the tracer until these concentrations stabilize at the injected values. Then, water without tracer is injected to flush the mobile polymer and tracer from the porous medium. Next, a second bank is injected that contains the same concentration of polymer and tracer as in the first bank, and the effluent polymer and tracer concentrations are again monitored until stabilization at the injected values. *IAPV* is then calculated using Eq. 1

$$IAPV = [\Sigma\ [(C_p/C_{po} * \Delta PV) - (C_t/C_{to} * \Delta PV)]] \quad \text{.....(1)}$$

where C_p is effluent polymer concentration, C_{po} is injected polymer concentration, C_t is effluent tracer concentration, C_{to} is injected tracer concentration, PV is the volume in one pore volume, ΔPV is pore-volume increment. In Eq. 1, the only data used is associated with arrival of the polymer and tracer fronts at the core exit for the second polymer/tracer bank. As illustrated in Figure 1, Eq. 1 measures *IAPV* as the area between the polymer and tracer breakout curves associated with the second polymer/tracer bank.

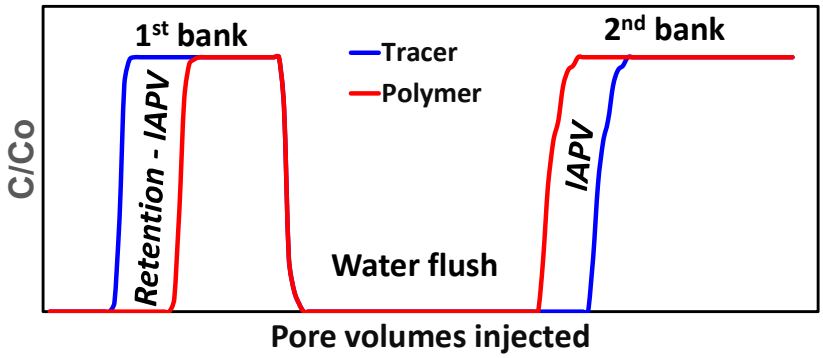

Figure 1—Illustration of the double polymer/tracer bank method to determine *IAPV* and retention.

Polymer retention can then be quantified as the area between the tracer and polymer breakout curves associated with the first polymer/tracer bank, as calculated using Eq. 2.

$$R_{pret} = \{[\Sigma\ [(C_p/C_{po} * \Delta PV) - (C_t/C_{to} * \Delta PV)]] + IAPV\} * C_{po} * PV / M_{rock} \quad \text{.....(2)}$$

where R_{pret} is polymer retention, and M_{rock} is the rock mass in the porous medium.

Inconsistencies from previous measurements. As demonstrated by Manichand and Seright (2014), Wang et al. (2021), and Seright and Wang (2023a), *IAPV* measurements reported in the petroleum literature have been notoriously inconsistent, with no correlation evident between *IAPV* and polymer size, molecular weight, or permeability of the porous medium. Gilman and MacMillan (1987) and Wang et al. (2021) demonstrated that *IAPV* can be substantially overestimated if (1) the tested core is heterogeneous or (2) especially, if insufficient water is flushed through the core between the two polymer banks. When water displaces polymer solution, viscous fingers or channels bypass polymer associated with the first polymer bank of the double polymer/tracer bank method. Unless a very large volume of water is flushed (perhaps 100 *PV* or more), mobile polymer will remain in the core when water injection stops. When the subsequent second polymer is injected, the remaining mobile polymer from the first polymer bank is efficiently displaced to the core outlet—falsely giving the impression that polymer from the second bank is exhibiting *IAPV*. Incidentally, Akbari described a number of variations that have previously advocated to measure *IAPV* (Akbari et al. 2019). All of these methods utilize a water post flush and can be compromised by viscous fingering of water through the polymer bank.

Doubt about interpretation of previously measured *IAPV* values also arises from consideration of the size of polymer molecules in solution, relative to the size of pores and pore throats. For common HPAM polymers used in enhanced oil recovery (e.g., 15-20 million g/mol Mw), molecular size in solution typically ranges from 0.1 to 0.5 μm, depending on salinity (Jouenne and Levache 2020; Seright et al. 2025). X-ray computed microtomography studies (Seright et al. 2006, 2009) demonstrated that over 98% of the pore throats and pore bodies in 470-mD Berea sandstone have effective radii greater than 5 μm (10-50 times the polymer radius). Consequently, virtually all pores in moderated-to-high-permeability (i.e., greater than 500 mD) sand and sandstone should be quite accessible to typical HPAM molecules. Since virtually all large-scale polymer floods comprise of sands and sandstone with permeability larger than 500 mD (Seright and Wang 2023b; Azad and Seright 2025), *IAPV* values less than 2% might be expected in most existing polymer-flooded reservoirs.

Perhaps indicating a lack of confidence in laboratory measurements, some simulators use *IAPV* as an adjustable parameter for history matching (Skoreyko and Kumar 2017). For those cases, it might be more appropriate to call the adjustable parameter a "simulation fudge factor" rather than misleadingly label it as *IAPV*.

The method of Dean et al. (2022). To circumvent viscous fingering associated with water displacing polymer during the double polymer/tracer method (and other previous methods), Dean et al. (2022) advocated injecting a bank with moderate polymer concentration/viscosity, followed by a bank with higher polymer concentration/viscosity **(Figure 2**). Both polymer banks must be large enough so that the effluent concentrations reach the injected concentrations (of polymer and tracer). After normalizing the baselines for the two banks, *IAPV* is established using the second-(high-concentration)-bank polymer breakout curve. The method assumes that polymer retention and *IAPV* are not functions of polymer concentration. The concept has considerable merit in its simplicity and avoidance of viscous-fingering problems associated with other methods for determining *IAPV*. However, additional examination is required because very few reports utilizing the method have been published (Dean et al. 2022), and important details about those tests (e.g., permeability, character of the rock, polymer concentrations) were not disclosed.

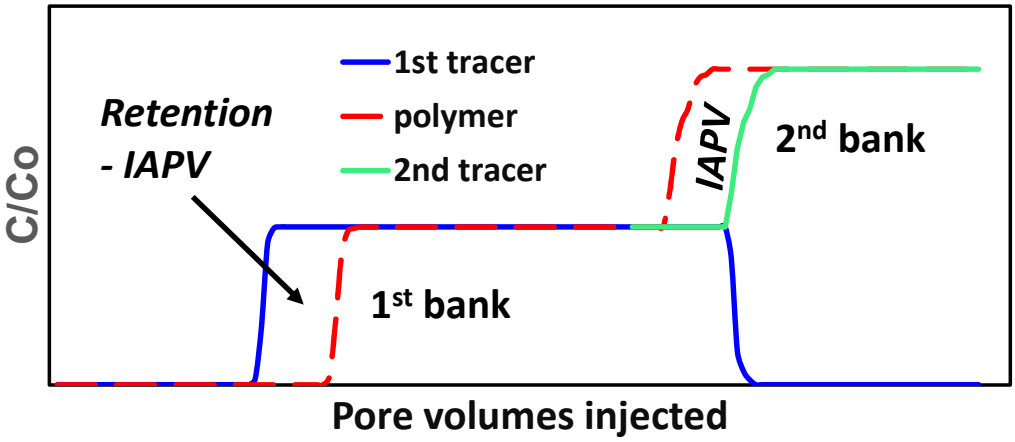

Figure 2—Illustration of method of Dean et al. (2022) to determine *IAPV* and retention.

Consequently, the goal of this paper is to examine the method advocated by Dean et al. (2022). After describing the experimental methodology, polymer retention and *IAPV* values are reported for sandstone cores and bead packs with permeabilities ranging from 113 to 18600 mD, porosities ranging from 0.188 to 0.402, and core lengths ranging from 30.48 to 122-cm (1 to 4 ft). Many tests involved 500-ppm HPAM (with no KI tracer) displacing 250-ppm HPAM (with a KI tracer). However, three sets of tests made five replicate determinations of *IAPV* using successive polymer banks with HPAM concentrations starting at 62.5 ppm and doubling in stages to 2000 ppm. This procedure tested the reproducibility of the method and whether the *IAPV* measurement depended on HPAM concentration. Different methods for assigning an *IAPV* value will be compared, including (1) the area between polymer and tracer breakout curves, (2) the difference in pore volume (*PV*) throughput (between polymer and tracer) upon attaining an effluent concentration of 50% of the injected concentration, and (3) the difference in *PV* during first breakout of polymer ahead of tracer. Finally, the relevance of *IAPV* and the results to field applications will be discussed.

Materials and Methods

Brine, polymer and temperature. The brine used in this work contained 0.2% NaCl. The polymer was Flopaam 3630S™ HPAM, which the manufacturer (SNF) stated had a molecular weight of 18-20 million g/mol and 30% degree of hydrolysis. All experiments were performed at 20°C.

Porous media. The porous media used in this work included Berea sandstone cores and glass bead packs. Permeabilities ranged from 113 mD to 18.6 D, while porosity ranged from 0.188 to 0.402. **Table 1** lists properties of the cores and glass bead packs. Most of the cores and bead packs were 30.48-cm long and 2.54-cm in diameter. However, the 113-mD Berea core was 122-cm long, with a 3.81-

cm x 3.81-cm square cross-section. Most cores and packs were contained in a Hassler cell with 500-psi confining pressure. However, the 113-mD Berea core was cast in epoxy, which limited the pressure and flow rate that could be applied.

Table 1—Summary of porous media and *IAPV* results

Permeability, darcys	Porosity	Core length, cm	Core material	Retention, µg/g	*IAPV*, % *PV*
18.6	0.402	30.48	200-µm glass beads	0.18	0%
17.3	0.377	30.48	200-µm glass beads	0 to 16.6	-5.6 to 2.1%
1.01	0.255	30.48	Berea sandstone	19.8	0%
0.473	0.210	30.48	Berea sandstone	5.43 to 7.4	-1.6 to 4.7%
0.383	0.209	30.48	Berea sandstone	11.9	2.5%
0.209	0.199	30.48	Berea sandstone	0 to 26.3	-36.2 to 26.8%
0.113	0.188	122	Berea sandstone	46	44.6%

Typical flooding procedure. Each porous medium was saturated with 0.2% NaCl brine (without KI tracer) before being flooded with 5-10 *PV* of polymer solution. In most experiments, the Darcy velocity during flooding was 1.86 ft/d. In contrast, the 113-mD Berea core was flooded at 0.89 ft/d to ensure that the pressure across the epoxy-cast core never exceeded 60 psi (which might risk breaching the epoxy). Oil was not used in these experiments. In many experiments, the first polymer bank contained 250-ppm HPAM and 20-ppm KI (and 0.2% NaCl). Also, in many experiments, the first 250-ppm-HPAM polymer bank was immediately followed by a bank containing 500-ppm HPAM (and 0.2% NaCl) with no tracer. With this method, the "tracer" associated with the second, more viscous polymer bank was the absence of the 20-ppm KI. Flow was not stopped when switching from one polymer bank to the next. In particular, the (closed) flow line for the second polymer bank was pressurized to match the pressure of the core inlet pressure at the end of injection of the first polymer bank. Then a three-way valve was opened that switched from injecting 250-ppm HPAM to 500-ppm HPAM. This procedure eliminated pressure surges during the switch.

Flooding procedure with concentration variations. Tables 2, 3 and 4 list the injection sequence during the tests designed to examine how polymer concentration affected *IAPV* determination. For the experiment in Table 2 (in the 17.3-D 200-µm glass bead pack), after brine saturation, the first 5-*PV* polymer solution injected contained 62.5-ppm HPAM, 20-ppm KI and 0.2% NaCl. The second 5-*PV* polymer solution contained 125-ppm HPAM, 0.2% NaCl and no KI. In subsequent tests, the polymer concentration was doubled with each successive polymer bank, and the presence or absence of 20-ppm KI alternated from one bank to the next. Table 3 describes a similar experiment in the 473-mD Berea sandstone core, while Table 4 applies to the 209-mD Berea core.

Effluent analysis. Effluent from packs was analyzed by several methods. A water tracer (20-ppm potassium iodide) was routinely monitored using a Genesys 2™ spectrophotometer at a wavelength of 230 nm. Effluent polymer concentration was monitored by three methods: total organic carbon, total nitrogen, and viscosity. For total organic carbon, a Shimadzu TOC-L™ was used. Total nitrogen was measured using chemiluminescence with a Shimadzu TNM-L™ unit. Viscosity was measured at 7.3 s^{-1} (20°C) using a Vilastic VE™ rheometer. These measurements were made at 4-cm^3 increments for each effluent sample. For figures in this paper, effluent concentrations are reported relative to the injected values. Also, because nitrogen detection is the most reliable measure of HPAM concentration in our case, all effluent polymer concentrations reported in this paper are based on that method.

Table 2—Effect of HPAM concentration on *IAPV* in 17.3-D 200-µm glass beads.

HPAM, ppm	KI, ppm	NaCl, %	Darcy velocity, ft/d	*PV* injected	Viscosity, cp @ 7.3 s^{-1}	Cumulative retention, µg/g	*IAPV*, % *PV*
0	0	0.2	1.86	10	0.9	--	--
62.5	20	0.2	1.86	5	1.3	0.00	--
125	0	0.2	1.86	5	2.6	0.00	2.1
250	20	0.2	1.86	5	5.2	1.13	-3.3
500	0	0.2	1.86	5	11.2	4.6	-5.1
1000	20	0.2	1.86	5	26.5	12.9	-5.6
2000	0	0.2	1.86	5	87.0	16.6	-1.4

Table 3—Effect of HPAM concentration on *IAPV* in a 473-mD Berea core.

HPAM, ppm	KI, ppm	NaCl, %	Darcy velocity, ft/d	*PV* injected	Viscosity, cp @ 7.3 s^{-1}	Cumulative retention, µg/g	*IAPV*, % *PV*
0	0	0.2	1.86	10	0.9	--	--
62.5	20	0.2	1.86	8	1.3	5.43	--
125	0	0.2	1.86	8	2.6	5.43	4.7
250	20	0.2	1.86	7	5.2	5.43	3.7
500	0	0.2	1.86	7	11.2	5.43	1.6
1000	20	0.2	1.86	7	26.5	5.43	4.3
2000	0	0.2	1.86	7	87.0	7.4	-1.6

Table 4—Effect of HPAM concentration on *IAPV* in a 209-mD Berea core.

HPAM, ppm	KI, ppm	NaCl, %	Darcy velocity, ft/d	*PV* injected	Viscosity, cp @ 7.3 s^{-1}	Cumulative retention, μg/g	*IAPV*, % *PV*
0	0	0.2	1.86	10	0.9	--	--
62.5	20	0.2	1.86	8	1.3	0	26.8
125	0	0.2	1.86	8	2.6	0	15.2
250	20	0.2	1.86	7	5.2	0.74	-5.2
500	0	0.2	1.86	7	11.2	11.1	-36.2
1000	20	0.2	1.86	7	26.5	11.1	1.2
2000	0	0.2	1.86	7	87.0	26.3	-13.2

In Tables 2-4, the retention column reports cumulative polymer retention. If the *IAPV* is positive for injection of a given polymer concentration, no additional retention is added to the retention value listed for the previous polymer injection. However, if the *IAPV* value is negative, that value is converted to an additional polymer retention value and added to the retention value listed for the previous polymer injection listing.

Results

Prior to this study, polymer retention and *IAPV* were normally determined using the double polymer tracer method (Lotsch et al. 1985; Wang et al. 2021; Seright and Wang 2022,2023a). By comparing with the current work, determination of *IAPV* using the method of Dean et al. (2022) was found to be far easier and faster to apply reliably than the standard double polymer/tracer method—primarily because it eliminates the need for a very large, time-consuming water bank between injection of the two polymer banks. Also, because the second polymer bank is more viscous than the first, it reduces uncertainty associated with water forming channels or viscous fingers through the first polymer bank.

18.6-D 200-μm glass bead pack. Figure 3 shows effluent tracer and polymer concentrations (relative to injected concentrations) for injection into the 18.6-D pack of 200-μm glass beads (Interactivia #7 grit). (These beads had a very narrow size distribution, as shown in Figure 12 of Seright and Wang 2022). During the first bank of polymer/tracer injection (250-ppm HPAM, 20-ppm KI), the polymer (dashed red curve in Figure 3) and tracer (solid green curve) arrived in the core effluent at the same time and rapidly increased to the injected concentration. After 5 *PV* of 250-ppm HPAM, 5 *PV* of 500-ppm HPAM was injected. Since the 500-ppm HPAM solution contained no KI tracer, the effluent KI concentration dropped to zero after injecting about 1 *PV* (blue curve). For polymer, the previous 250-ppm HPAM concentration was taken is the new "zero" baseline for the second bank, so the dashed black curve in Figure 3 shows the jump in effluent polymer concentration after injecting about 1 *PV* of 500-ppm HPAM. Figure 3 reveals that effluent concentrations stabilized quite quickly after injecting about 1 *PV* of a given polymer/tracer concentration.

Figure 4 replots Figure 3, with a focus on the transitions from one injected polymer concentration to the next. The green and red curves are plotted in the same way as in Figure 3. However, the blue curve from Figure 3 is inverted (going from 0 to 1 instead of from 1 to 0). Thus, for this case, 20-ppm KI was taken as the "zero" baseline, and 0-ppm KI was assigned as full injected concentration of the "tracer". Also, for the blue curve in Figure 4 subtracts 5 *PV* from the throughput in Figure 3, so that the tracer curves from the first and second polymer banks can be compared more closely. This subtraction was also applied to the second-bank polymer data from Figure 3, so that the polymer curves from the two banks can be compared.

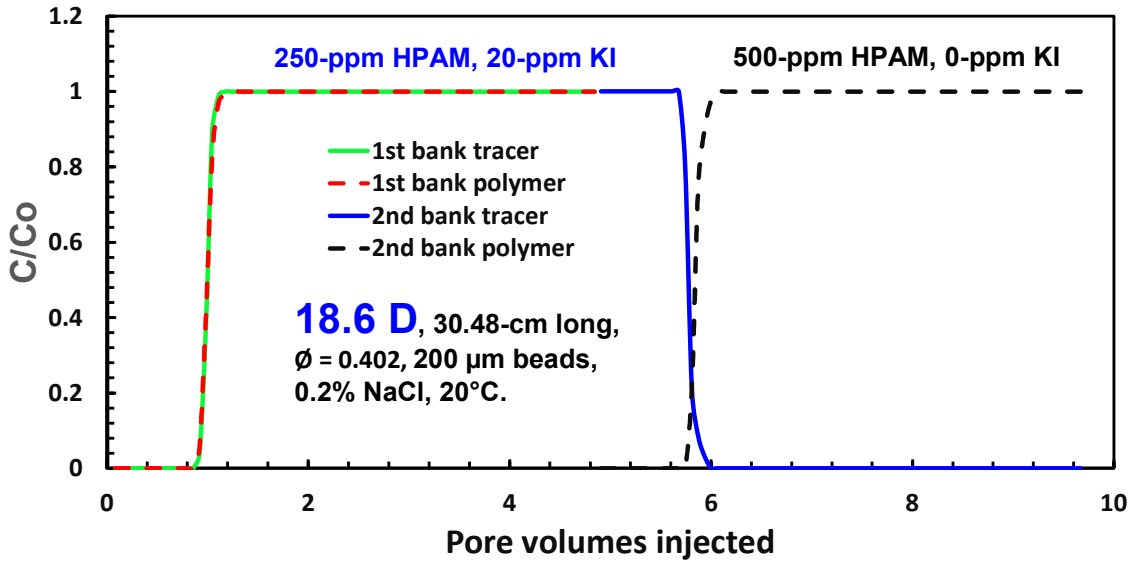

Figure 3—Polymer and tracer effluent concentrations for 18.6-D bead pack.

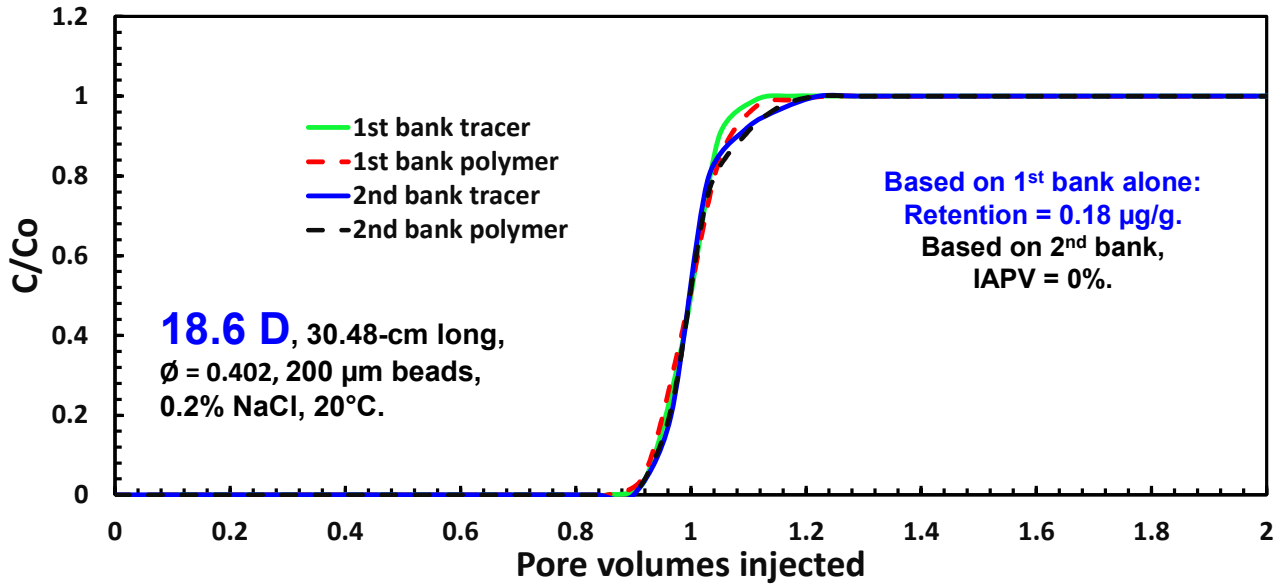

Figure 4—Re-plot of Figure 3, focusing on the transitions.

A comparison of the green and blue curves in Figure 4 reveals that breakout of the KI tracer for the first (250-ppm) polymer bank matched reasonably well with the "tracer" associated with the second (500-ppm) polymer bank. Thus, potassium iodide (and its subsequent displacement) acted as expected as a reproducible water tracer.

If *IAPV* is assumed to be zero, the difference in breakout between the first bank tracer and polymer breakout curves (the green and red curves in Figure 4) provide polymer retention. From Eq. 2, a retention value of 0.18 µg/g was calculated. This very low value is not surprising since the porous medium was 200-µm glass beads.

For polymer breakout during the second bank (500-ppm HPAM), the dashed black curve in Figure 4 matches the other three curves quite closely. As expected, Eq. 1 calculates an *IAPV* value of zero. For closely packed uniform, 200-µm spherical glass beads, pore throats are (mathematically) expected to be in the range from 20 to 40 µm. Consequently, HPAM molecules with ~0.35-µm radius are not expected to experience a significant size-exclusion effect.

Effect of polymer concentration on *IAPV* determination.
The effect of HPAM concentration on *IAPV* determination was investigated. Three sets of experiments were performed—one using 17.3-D 200-µm glass beads; a second using a 473-mD Berea core; and a third using a 209-mD Berea core. As in other cases, the core was first saturated with 0.2% NaCl brine containing no potassium iodide. Next, many pore volumes of polymer solution were injected that contained 62.5-ppm HPAM, 20-ppm KI, and 0.2% NaCl. Effluent tracer and polymer concentration was monitored continuously. Then the sequences indicated in Tables 2, 3 and 4 were followed, injecting polymer banks of increasing concentration. The polymer concentration was doubled with each successive polymer bank, and the presence or absence of 20-ppm KI alternated from one bank to the next. Presumably, polymer retention of the core was satisfied during injection of the first (62.5-ppm HPAM) bank, while replicate *IAPV* determinations could be made during the subsequent five polymer banks.

Tracer consistency. Figures 5, 6 and 7 compare tracer breakout curves associated with the six polymer injection steps of these three experiments. Recall that the tracer is 20-ppm KI for the 62.5-ppm, 250-ppm, and 1000-ppm HPAM cases, while the 125-ppm, 500-ppm, and 2000-ppm HPAM cases used the absence of KI as a tracer. With the minor exception of the 1000-ppm-HPAM case in Figure 6, the various tracer curves overlap quite closely for a given experiment. These results indicate that 20-ppm KI (and its absence) functioned extremely reproducibly as a water tracer. In the 200-µm glass beads (Figure 5), the tracer breakout curves were quite sharp—with first tracer breakout occurring after 0.9 *PV* and full injection concentration reached by 1.1 *PV*. In Berea sandstone, tracer breakout was a bit more disperse—with first tracer breakout occurring after 0.8 *PV* and tracer injected concentration reached about 1.2-1.3 *PV* (Figures 6 and 7).

Polymer breakout curves versus concentration. Figure 8 plots the polymer breakout curves associated with the data in Figure 5 and Table 2; **Figure 9** plots polymer breakout curves associated with the data in Figure 6 and Table 3; while **Figure 10** plots polymer breakout curves associated with the data in Figure 7 and Table 4. Although many pore volumes of polymer solutions were injected during each step, these figures stop at 2 *PV* (or 5 *PV* in the case of Figure 10) to highlight the changes observed. For reference, the blue dashed curve plots a tracer breakout curve. The solid blue curve plots the first breakout of polymer, during injection of 62.5-ppm HPAM.

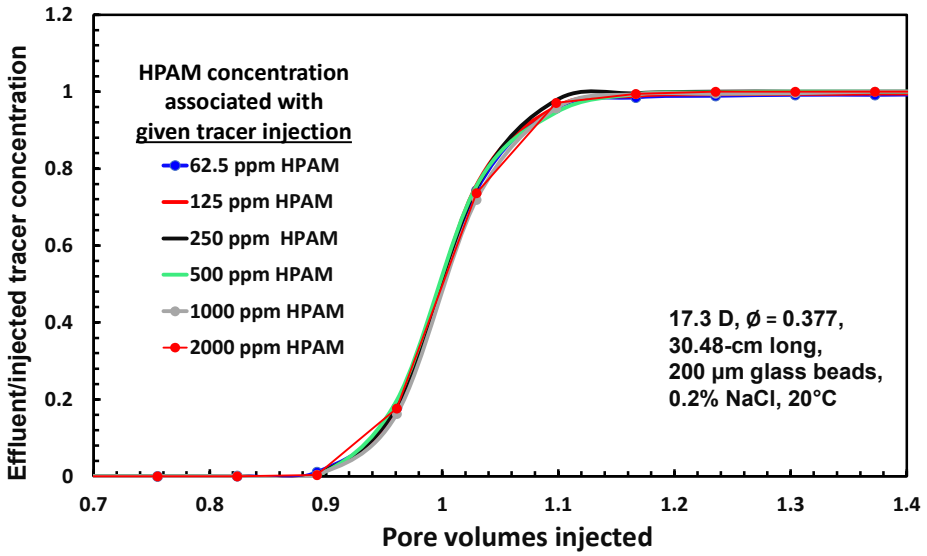

Figure 5—Comparison of tracer breakout curves in the 17.3-D glass bead pack.

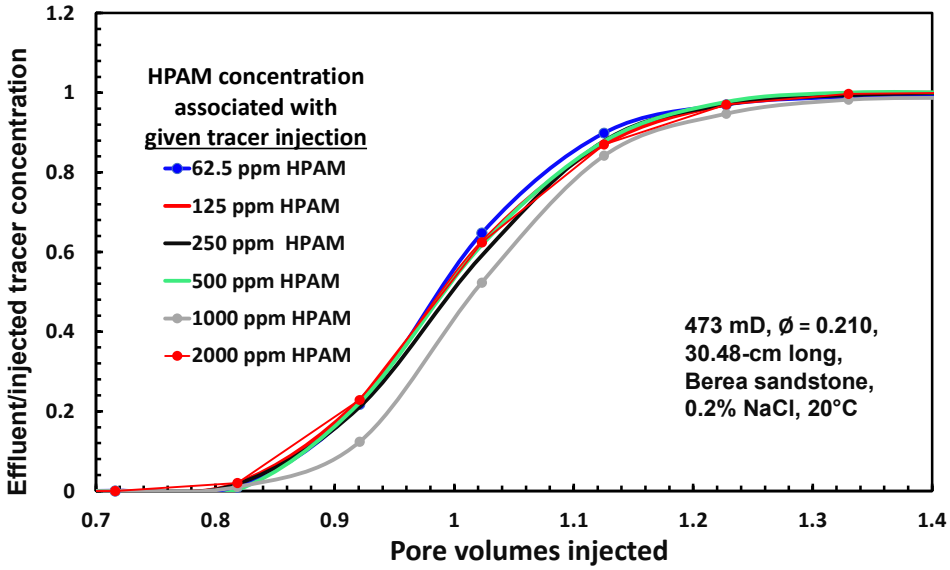

Figure 6—Comparison of tracer breakout curves in the 473-mD core.

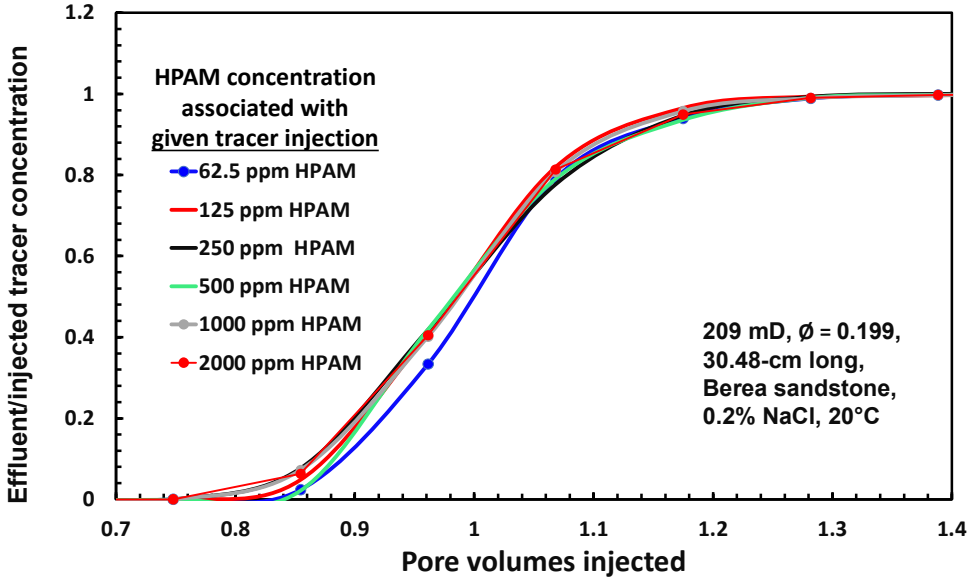

Figure 7—Comparison of tracer breakout curves in the 209-mD core.

17.3-D 200-µm glass bead pack. For Figure 8, using Eq. 2 and the first polymer injected (62.5-ppm HPAM), polymer retention was 0.00 µg/g, which is not surprising since the pack consists of uniform 200-µm glass beads. A close look at the tracer (blue dashed) curve and the 62.5-ppm-HPAM curve reveals that the polymer broke out slightly earlier than the tracer, but the polymer lagged the tracer for a small section in the upper concentrations. The 50%-concentration level was reached at the same time for both tracer and 62.5-ppm HPAM. Thus, the zero-polymer retention resulted from a trade-off from the upper and lower parts of the curves.

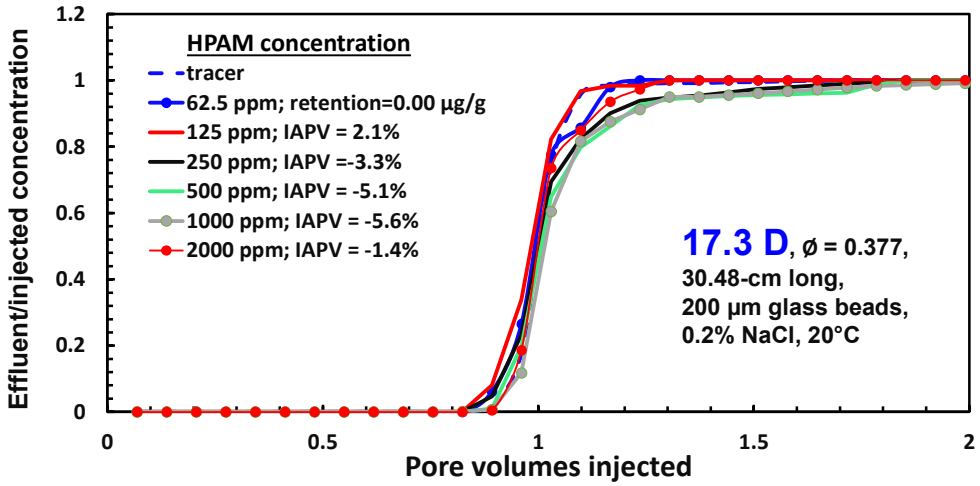

Figure 8—Comparison of polymer breakout curves in the 17.3-D glass bead pack.

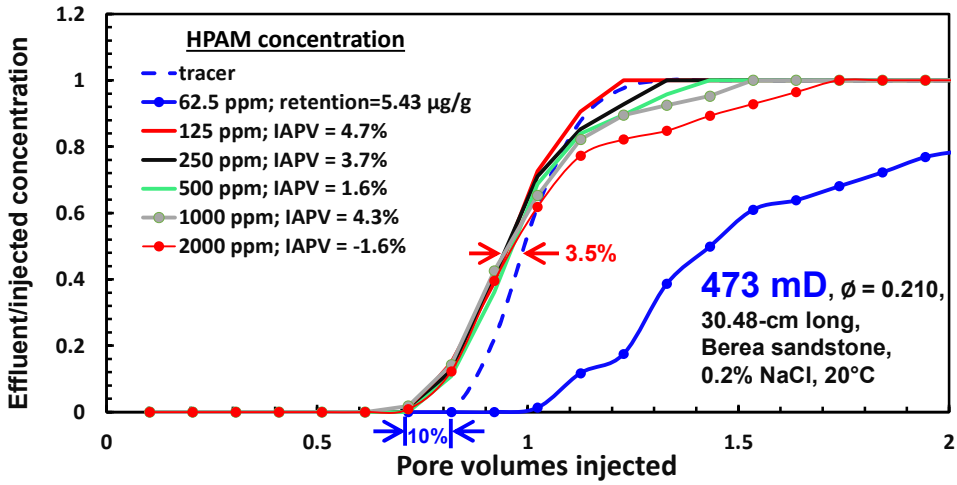

Figure 9—Comparison of polymer breakout curves in the 473-mD core.

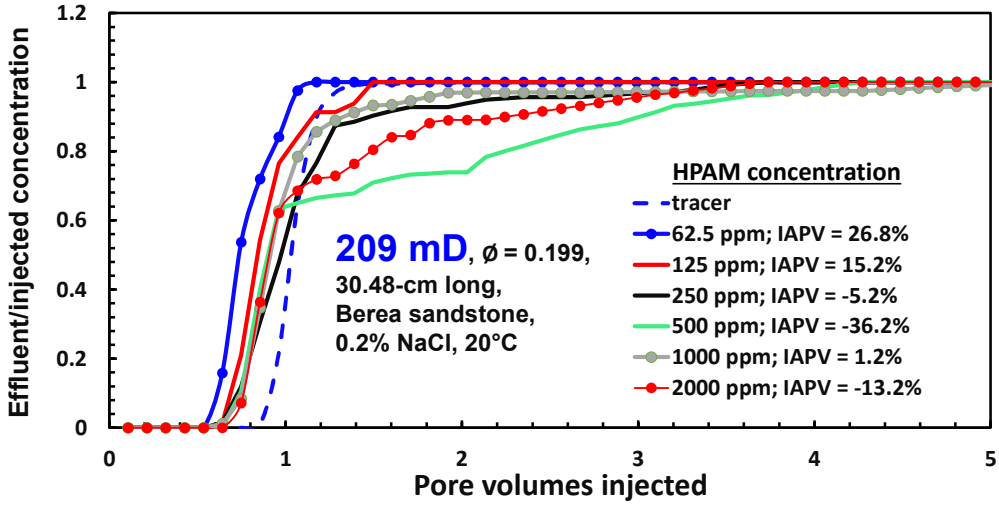

Figure 10—Comparison of polymer breakout curves in the 209-mD core.

In Figure 8 for most concentrations, polymer first arrived in the pack effluent at about the same time as the tracer, although if one wanted to nitpick, it might be said that the 62.5-ppm, 125-ppm, and 250-ppm polymer arrived very slightly ahead (i.e., ~0.85 *PV*) of the tracer and 500-ppm, 1000-ppm and 2000-ppm cases (~0.9 *PV*). The 50%-concentration level was reached at 1 *PV* for the tracer and all polymer cases. Thus, if reaching the 50%-concentration level was the criterion for assessing *IAPV*, one could argue that the *IAPV* was zero for the cases where HPAM concentration was 2000 ppm or less. This is not surprising, since the minimum opening size in these uniform 200-μm glass beads is about 20 μm—compared to ~0.35 μm for a typical 20-million-g/mol HPAM molecule in solution.

Interestingly, if Eq. 1 is formally used to calculate *IAPV*, the *IAPV* values appear to decrease with increased HPAM concentration—from 2.1% to negative 5.6% as polymer concentration increases from 125 ppm to 1000 ppm. A negative *IAPV* value is equivalent to polymer retention being greater during injection of the more-concentrated second polymer bank than during the first polymer bank. If the porous medium exhibits significant retention, the results might be attributed to concentration-dependent adsorption (Zhang and Seright 2014). However, it seems unlikely that any significant adsorption occurs on 200-μm glass beads (see the first two data rows of Table 1). Thus, one might argue that the *IAPV* range from -5.6% to 2.1% simply reflects experimental variation for this case.

473-mD Berea sandstone core. Figure 9 shows polymer breakout curves for the 473-mD Berea core. Assuming *IAPV* =0, Eq. 2 calculates a polymer retention value of only 5.43 μg/g. The solid red curve with no symbols illustrates polymer breakout during injection of 125-ppm HPAM to provide the first measure of *IAPV*. From Eq. 1, the data yielded an *IAPV* of 4.7%. The black, green, grey, and red-dot curves show polymer breakouts during subsequent injection of 250-ppm, 500-ppm, 1000-ppm, and 2000-ppm HPAM—yielding *IAPV* values of 3.7%, 1.6%, 4.3%, and negative 1.6%, respectively.

For all five of the *IAPV* curves in Figure 9 (i.e., 125-ppm to 2000-ppm HPAM), polymer first arrived at the core outlet at 0.7 *PV*—compared to slightly over 0.8 *PV* for the tracer. Also, these five curves closely overlapped and were to the left of the tracer curve up to 0.5 *PV*. Consequently, below 0.5 *PV*, one could argue that *IAPV* accelerated HPAM propagation by about 10% at first polymer breakout, but that effect diminished to about 3.5% by 0.5 *PV*. Beyond 0.5 *PV*, the five curves diverged, with the extent of delay or "tailing" increasing with increased polymer concentration. Thus, in contrast to the behavior before 0.5 *PV*, the polymer generally propagated slower than the tracer after 0.5 *PV*. The 125-ppm-HPAM curve most closely matched the tracer curve. As shown in Figure 9 and Table 3, *IAPV* values can be calculated (using Eq. 1) for these curves—with values ranging from -1.6% to 4.7%. However, it is arguable whether the effects seen are necessarily due to size-exclusion.

A message from Figure 9 might be that *IAPV* assessments made using lower polymer concentrations are more likely to be credible than using higher polymer concentrations.

209-mD Berea sandstone core. Figure 10 shows polymer breakout curves for the 209-mD Berea core. Assuming *IAPV* =0, Eq. 2 calculates a polymer retention value of about *negative* 2 μg/g. Put another way, if retention is assumed to be zero, Eq. 1 projects that the *IAPV* is 26.8%. As indicated in Figure 10, *IAPV* projections for the subsequent polymer banks yield values of 15.2%, negative 5.2%, negative 36.2%, positive 1.2% and negative 13.2% for polymer concentrations of 125 ppm, 250 ppm, 500 ppm, 1000 ppm, and 2000 ppm, respectively. As mentioned earlier, negative *IAPV* values indicate additional polymer retention. With *IAPV* values ranging from negative 36% to positive 26.8%, an *IAPV* assignment of zero might be as appropriate as any other value for this 209-mD core.

From Figure 10, first polymer breakout occurred at 0.54 *PV* when injecting 62.5% HPAM, compared to first tracer breakout at 0.85 *PV*. For the other five polymer banks, first polymer breakout occurred at 0.64 *PV.* Thus, as for the 473-mD case above (Figure 9), first polymer breakout occurred notably earlier than first tracer breakout, and (except for the 62.5-ppm case) first polymer breakout was not dependent on polymer concentration. If *IAPV* was assigned strictly on first polymer breakout, one might argue that *IAPV* in 209-mD Berea was 21% (e.g., 0.85 minus 0.64). This assignment would be double that for the 473-mD Berea core (Figure 9).

In Figure 10, a notable "tailing" phenomenon occurred for many of the polymer banks—where a substantial number of pore volumes must be injected for the effluent to achieve the injected polymer concentration. This "tailing" was drawn out over 5 PV for some polymer concentrations—substantially longer than observed in the 473-mD case (Figure 9). Interestingly, the most prominent tailing in Figure 10 occurred with the 500-ppm case (solid green curve). This observation suggests that polymer retention in Berea is most sensitive to concentration around 500-ppm HPAM. This suggestion is consistent with Figure 7 of Zhang and Seright (2014). Incidentally, "tailing effects" (such as those show here) were extensively investigated previously and attributed to the presence of clays (especially, kaolinite and illite) (Wang et al. 2021; Seright and Wang 2022,2023a).

If *IAPV* was based on achieving a polymer concentration that was 50% of the injected value, *IAPV* would be close to zero for the cases in Figure 8 (17.3-D beads). For Figure 9 (473-mD Berea), the 50%-concentration-level *IAPV* was about 3.5% for all cases. For Figure 10 (209-mD Berea) the 50%-concentration-level *IAPV* was about 15% for the 500-, 1000-, and 2000-ppm cases, but varied from 7% to 25% for the 62.5-, 125- and 250-ppm cases.

For comparison, if *IAPV* was based on the difference between the first polymer arrival and the first tracer arrival, *IAPV* would be close to zero for the cases in Figure 8 (17.3-D beads), about 10% for 473-mD Berea (Figure 9), and about 20% for most of the cases (excluding the 62.5-ppm case) in 209-mD Berea (Figure 10).

Which *IAPV* value should be used? In the vast majority of cases *IAPV* is used as an input parameter during simulations or fractional flow calculations to assess the efficiency with which injected polymer displaces oil. Those calculations are dominated by the polymer properties at the highest polymer concentrations. This realization indicates that the formally accepted method of determining *IAPV* (i.e., Eq. 1) should be applied. (However, we noted that the form of the actual polymer breakout curves may be substantially different from those symmetrical forms assumed during simulations of polymer flooding.) Polymer viscosity at low concentrations (i.e., first polymer breakout or achieving 50% of the injected concentration) do not contribute as significantly to enhancing oil displacement. During polymer flood simulations or fractional flow calculations, the *IAPV* parameter is input in a form such that higher *IAPV* values accelerate the movement of the full-polymer-concentration polymer and the displacement of oil. However, the behavior in the 209-mD core (Figure 10) is clearly not consistent with the *IAPV* form that is assumed as input during simulations or fractional flow calculations, and it is clearly not accelerating the movement of the highest polymer concentrations. Thus, the *IAPV* concept may be inappropriate and largely meaningless from the viewpoint of improving sweep efficiency in rock such as 209-mD Berea sandstone.

One might speculate that concentration-dependent *IAPV* values occur because of increased polymer entanglements and network formation at higher HPAM concentrations—suggesting that entangled polymers effectively make a gel particle that is too large to pass through some pore throats. However, the available evidence (De Gennes 1979; Seright et al. 1981.2025) reveals that these entanglements are too weak for this suggestion to be viable. [Further, if this explanation was valid, first polymer breakout in Figures 9 and 10 should not have been independent of polymer concentration (from 125-2000 ppm).] At any rate, the results suggest caution when assessing *IAPV* using these types of experiments and especially, the current methods of applying the results to prediction of acceleration of polymer and oil banks during a polymer flood.

Could the tailing effect be caused by something other than polymer retention or inaccessible pore volume? In particular, could the behavior be due to polymer rheology coupled with heterogeneity in the porous medium? Consider a two-layer porous medium where free crossflow can occur between two layers. Previous work (Seright 1991; Sorbie and Seright 1992; Seright 2010) demonstrated that if a viscous polymer solution displaces water, any common polymer rheology (i.e., Newtonian, shear-thinning, shear-thickening) will improve displacement efficiency (i.e., make the polymer front travel farther in the less-permeable layer, relative to the more-permeable layer). In contrast, if the two-layered porous medium is completely filled with a shear-thinning fluid (as is the case for the second and subsequent polymer banks in our *IAPV* experiments), the velocity contrast (v_1/v_2) is proportional to the permeability contrast (k_1/k_2) raised to a certain power. If that power is 1.5 (which may be common for somewhat concentrated polymer solutions in enhanced oil recovery, and if the permeability contrast is 10 to one (Seright 2010), the fluid velocity would be 32 times greater in the high-permeability layer than in the less-permeable layer. Thus, one might suspect this effect of providing an apparent acceleration of the more concentrated polymer through the most-permeable pathway. However, one would expect an equivalent acceleration of the tracer—which clearly did not happen in any of the figures in this paper. Also, if there was a significant heterogeneity to the bead pack or core, the effluent tracer concentration should have exhibited a notable tail (as tracer gradually was produced from the less-permeable pathways). The fairly sharp and symmetric tracer breakout curves shown in this paper argue against the existence of any significant heterogeneity.

Figure 11 (after Figure 5 of Sorbie and Seright 1992) illustrates how cross-flow between high- and low-permeability pathways could result in a tailing effect when a more-viscous fluid displaces a less-viscous fluid. Crossflow from Layer 1 into Layer 2 creates the angled red-blue interface in Layer 2. When the polymer front reaches the core outlet, a concentration tailing phenomenon will be observed as more polymer arrives from Layer 2 with increased throughput. However, as with the previous argument, if this scenario was valid, the produced tracer profile should also have exhibited the tailing phenomenon. Again, since all the produced tracer profiles were sharp and exhibited no sign of tailing, the presence of significant heterogeneity seems unlikely.

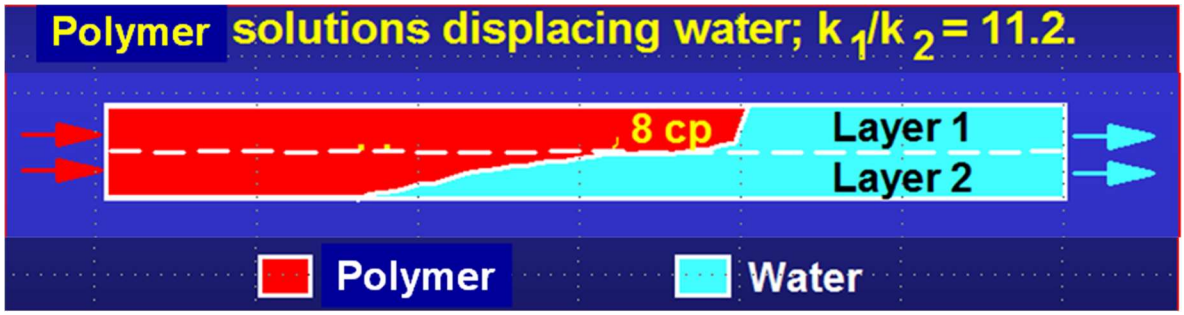

Figure 11—Possible rheology origin of tailing effect. After Figure 5 of Sorbie and Seright 1992.

***IAPV* in sandstones with other permeabilities**

383-mD Berea sandstone core. Figure 12 shows the results of *IAPV* experiments in 383-mD Berea sandstone. In this experiment, seven *PV* of 250-ppm HPAM (with 20-ppm KI tracer) was followed by seven *PV* of 500-ppm HPAM (without KI tracer). The solid blue and green curves demonstrate that the tracer breakout curve during the second polymer bank matched well with the tracer curve

during the first polymer bank. The dashed red curve shows HPAM breakout during the first polymer injection bank, which ultimately (after accounting for 2.5% *IAPV*) yielded a polymer retention value of 11.9 µg/g.

Different ways to calculate *IAPV*. The dashed black curve shows HPAM breakout during the second polymer bank. Similar to the 500-ppm-HPAM case in Figure 9, the polymer first arrived at the core outlet after 0.7 *PV*, which again, was earlier than the first tracer arrival (at ~0.9 *PV*). Thus, if *IAPV* were defined as the difference between first polymer breakout and first tracer breakout, *IAPV* would be about 20%. The second-bank HPAM curve remained to the left of the tracer curve until about 1 *PV*, after which the HPAM curve lagged significantly from the tracer curve. If attaining 50% of the injected concentration was used as the criterion, IAPV would be 9%. In contrast, Eq. 1 calculates an *IAPV* of 2.5%, but it is arguable how much size-exclusion contributes to the behavior observed. In particular, there may be difficulty envisioning that size-exclusion accounts for the lower-than-expected HPAM concentrations (in the second polymer bank) after 1 *PV*. If one only considers the area where the second polymer bank (the black dashed curve in Figure 12) is to the left of the second tracer bank (the solid blue curve), the *IAPV* value would be 10.4%. In that case, the area where polymer concentrations were less than the tracer concentrations (i.e., to the right of and under the blue curve but above the black dashed curve) yields a polymer retention of 3 µg/g associated with the second polymer injection.

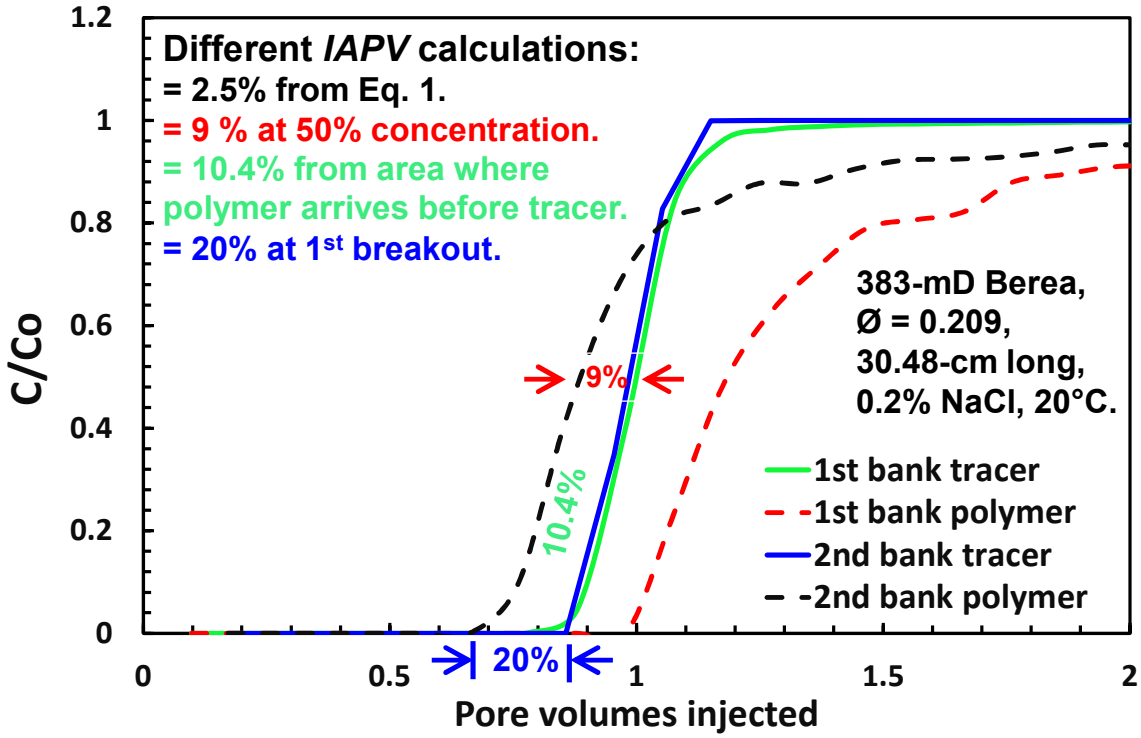

Figure 12—*IAPV* determination in a 383-mD core.

113-mD Berea sandstone core. Figure 13 shows the results of *IAPV* experiments in 113-mD Berea sandstone. In this experiment, 4.2 *PV* of 250-ppm HPAM (with 20-ppm KI tracer) was followed by 5 *PV* of 500-ppm HPAM (without KI tracer). This 122-cm long core had a large pore volume (334 cm^3), which allowed effluent samples to be collected every 1% *PV* (compared to ~10% *PV* for the studies described above). The dashed red curve shows HPAM breakout during the first polymer injection bank, which ultimately (after accounting for 44.6% *IAPV*) yielded a polymer retention value of 46 µg/g. If *IAPV* was assumed to be zero, HPAM retention would have been 24 µg/g. As with all experiments reported in this paper, after tracer breakthrough, no face plugging or gradual rise in pressure was observed during the course of polymer injection. Further, no accumulation of polymer or gel was noted on the inlet or outlet core faces at the end of the experiment.

The dashed black curve shows HPAM breakout during the second polymer bank. Interestingly, for this case, the polymer breakout was definitively ahead of the tracer breakout at all times, and the polymer "tailing" effect seen in Figures 9, 10, and 12 was not evident. The calculated *IAPV* was 44.6% using Eq. 1, 43% based on attaining 50% effluent concentration, and 36% based on first breakout. These values are high but not unreasonable, considering the low-permeability of the core.

Others have understandably asserted that low-permeability rocks may possess a significant fraction of pores that are not accessible by high-Mw polymers, especially carbonates that have a bimodal pore size distribution. For example, Souayeh et al. (2022) reported *IAPV* values up to 68% in 200-300-mD Indiana limestone where 56% of the pores were below 1 µm. Interestingly, Song et al. (2022) observed *IAPV* values from 0-11% in <50-mD Edwards Yellow limestone cores where 90% of the pore throat openings were between 1 and 10 µm.

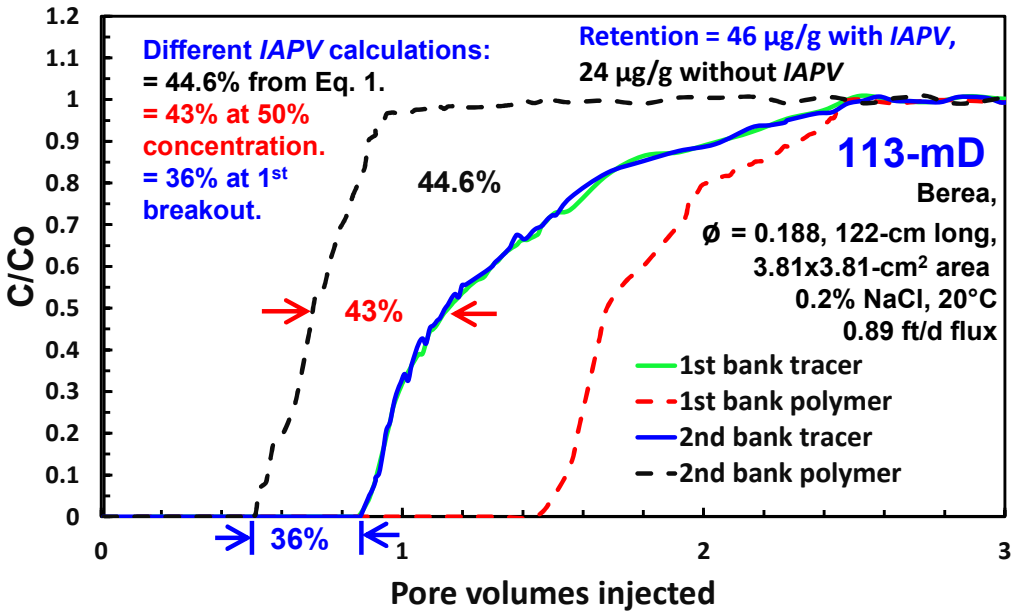

Figure 13—*IAPV* determination in a 113-mD core.

Discussion

Our experience with the method of Dean et al. (2022) reveals that it is substantially easier, faster and more reliable for determining *IAPV* than the double polymer-tracer-bank method (Lotsch et al. 1985). Past analysis (Manichand and Seright 2014; Wang et al. 2022; Seright and Wang 2024) revealed that few people have the patience to inject a sufficiently large brine bank when using the double polymer-tracer-bank method.

That being said, even with the superior method of Dean et al. (2022), substantial uncertainties arise from assessments of *IAPV*—notably, in rock with permeability above 200 mD. As demonstrated during the discussion of Figures 9, 10 and 12, there are multiple methods that could be used to assign an *IAPV* value, including (1) the formally accepted method of Eq. 1, (2) the difference in *PV* (between polymer and tracer) upon attaining an effluent concentration of 50% of the injected concentration, and (3) the difference in *PV* during first breakout of polymer ahead of tracer. The figures in this paper revealed significant differences in calculated *IAPV* values for these methods.

A curious result from Figures 9, 10 and 12 is that during the second (or subsequent) banks of polymer injection, the effluent polymer concentration commonly fell below the tracer concentration (relative to the injected concentrations) during part of the injection process. One interpretation of this result was that polymer retention varied with polymer concentration (in violation of a key assumption in the method of Dean et al. 2022). This interpretation is consistent with reports from Zhang and Seright (2014) for the range of polymer concentrations tested in this work. Nevertheless, in Figures 9, 10 and 12, one wonders why some level of apparent *IAPV* is seen upon first polymer breakout, but polymer retention/retardation is evident later at higher effluent concentrations. Figures 9 and 10 imply that if *IAPV* is based only on first polymer/tracer breakout, the *IAPV* is independent of polymer concentration (from 125 to 2000 ppm). One might rationalize that regardless of polymer concentration, the same fraction (e.g., 10-20%) of the largest polymer molecules travel rapidly through the most-permeable pathway (and presumably the largest pores) where the area for adsorption may be less than in less-permeable pathways. Subsequently, the remainder of polymer molecules displace less-concentrated polymer from the smaller pores, where concentration-dependent adsorption/retention becomes evident.

As mentioned above, the presence of true excluded volume effects is not surprising in low-permeability rock (e.g., less than 200 mD for 18-20-million g/mol HPAM). However, virtually all existing large-scale polymer floods occur in reservoirs where most of the rock/sand is more permeable than 500 mD (Seright and Wang 2023b; Azad and Seright 2025). (And all the existing large-scale polymer floods use HPAM with similar composition and Mw as that in this work.) Thus, it seems reasonable to question the need, the practicality and the value of utilizing the *IAPV* concept for these polymer floods. Of course, the suggested 200-mD limit (for applicability of the *IAPV* concept) applies here to HPAM with 18-20-million g/mol Mw, since that is the only polymer used in this work. Presumably, that limit might be raised for lower-Mw polymers and lowered for higher-Mw polymers.

As pointed out in the Introduction, some simulators use *IAPV* strictly as an adjustable parameter to facilitate their history matching. It would be more honest and functional to not label an adjustable parameter as *IAPV*. If improvements in the operation of the polymer flood are to be identified (e.g., changing the polymer Mw or polymer concentration or bank size), successful alterations are far more likely to result through insights from real physical phenomena, rather than unrealistic fiction.

The *IAPV* concept is primarily used during simulations and/or fractional flow calculations to judge whether and the extent of *IAPV* in accelerating the main body of the polymer bank and any oil bank through a reservoir during a polymer flood (Green and Willhite 1998). The input form of *IAPV* for these simulations/calculations commonly assumes that the polymer concentration will rapidly rise from low values to near-injection concentrations over a short distance around the polymer front (Green and Willhite 1998). These assumptions may not be consistent with the true form of polymer propagation (see Figures 9, 10, and 12 and the figures in Wang et al. 2021; Seright and Wang 2022,2023a)—thus, further compromising the *IAPV* concept for common medium-to-high-permeability applications.

From a practical viewpoint, would the actions mimicked during an *IAPV* laboratory experiment be relevant to a field application? In most polymer flood applications, polymer of a single concentration is injected, and the primary question is how rapidly will the polymer front propagate through the reservoir (and with what concentrations)? During laboratory testing, this question is addressed quite well during the first bank of polymer injection—either with the standard double polymer/tracer bank method or the method of Dean et al. (2022). However, does information collected beyond the first polymer bank provide unambiguous value? Based on this work and previous studies (Seright 2017; Wang et al. 2021), it is not clear that it does. As mentioned above in the section "Which *IAPV* value should be used?", from the viewpoint of reservoir engineering and sweep improvement (with 18-20-million g/mol HPAM in rock with >200-mD permeability), the *IAPV* concept appears inappropriate and largely meaningless in rock that shows the behavior seen in 209-, 383- and 473-mD Berea sandstone (Figures 9, 10 and 12).

Conclusions

1. The method of Dean et al. (2022) is substantially easier, faster and more reliable for determining *IAPV* than the double polymer-tracer-bank method (Lotsch et al. 1985).
2. Nevertheless, important uncertainties arise from assessments of *IAPV.* With a given data set, multiple methods can be used to assign an *IAPV* value, including (1) the area between polymer and tracer breakout curves (Eq. 1), (2) the difference in *PV* (between polymer and tracer) upon attaining an effluent concentration of 50% of the injected concentration, and (3) the difference in PV during first breakout of polymer ahead of tracer. Significant differences in calculated *IAPV* values were noted for these different methods.
3. During the second (or subsequent) banks of polymer injection for several experiments, the effluent polymer concentration commonly fell below the tracer concentration (relative to the injected concentrations) for part of the injection process. One interpretation of this result was that polymer retention varied with polymer concentration (in violation of a key assumption in the method of Dean et al. (2022). In 209-473-mD Berea, this interpretation is consistent with reports from Zhang and Seright (2014) for the range of polymer concentrations tested in this work.
4. From this work, it is arguable whether a significant *IAPV* exists in Berea sandstone or bead packs with permeability greater than 200-mD when using 18-20-million g/mol HPAM.
5. In most polymer flood applications, polymer of a single concentration is injected, and the primary question is how rapidly will the polymer front propagate through the reservoir (and with what concentrations)? During laboratory testing, this question is addressed quite well during the first bank of polymer injection—either with the standard double polymer/tracer bank method or the method of Dean et al. (2022). The value information (to planning of a field project) collected beyond the first polymer bank (during laboratory experiments) is debatable.

Nomenclature

C = effluent concentration, mg/L or ~ppm [μg/g]
C_o = injected concentration, mg/L or ~ppm [μg/g]
C_p = effluent polymer concentration, mg/L or ~ppm [μg/g]
C_{po} = injected polymer concentration, mg/L or ~ppm [μg/g]
C_t = effluent tracer concentration, mg/L or ~ppm [μg/g]
C_{to} = injected tracer concentration, mg/L or ~ppm [μg/g]
HPAM = partially hydrolyzed polyacrylamide or acrylamide-acrylate copolymer
IAPV = inaccessible pore volume
k = permeability, darcies [μm^2]
k_1 = permeability in Layer 1, darcies [μm^2]
k_2 = permeability in Layer 2, darcies [μm^2]
M_{rock} = mass of rock in the sand pack, g
M_w = polymer molecular weight, g/mol [daltons]
PV = pore volumes of fluid injected
ΔPV = pore volumes difference
R_{pret} = polymer retention, μg/g
v_1 = fluid velocity in Layer 1, ft/d [m/s]
v_2 = fluid velocity in Layer 2, ft/d [m/s]
ϕ = porosity

References

Akbari, S. Mahmood, S., Nasr, N., Al-Hajri, S. 2019. A Critical Review of Concept and Methods Related to Accessible Pore Volume during Polymer-Enhanced Oil Recovery. *J. Petroleum Science and Engineering* **182** 106263. doi: 10.1016/jpetrol.2019.106263.

Azad, M., Seright. R.S. 2025. Are Field Polymer EOR Projects Reaping the Benefits of SOR Reduction Due to Polymer Viscoelasticity? *SPE Journal* **30**. doi:10.2118/223155-PA.

Chauveteau, G. 1981. Molecular Interpretation of Several Different Properties of Flow of Coiled Polymer Solutions Through Porous Media in Oil Recovery Conditions." Paper 10060 presented at the SPE Annual Technical Conference and Exhibition, San Antonio, Texas, October 1981. doi: https://doi.org/10.2118/10060-MS.

Dawson, R., and Lantz, R.B. 1972. Inaccessible Pore Volume in Polymer Flooding. *SPE Journal* **12** (5): 448–452. doi: 10.2118/3522-PA.

Dean, R.M., Britton, C.J., Driver, J.W., Pope, G.A. 2022. State-of-the-Art Laboratory Methods for Chemical EOR. Paper SPE 209351 presented at the SPE Improved Oil Recovery Conference, Virtual, April 2022. doi: 10.2118/209351-MS.

De Gennes, P-G. 1979. Scaling Concepts in Polymer Physics. Cornell University Press. Ithaca.

Delamaide, E. 2014. Polymer Flooding of Heavy Oil - From Screening to Full-Field Extension. Paper SPE-171105-MS presented at the SPE Heavy and Extra Heavy Oil Conference: Latin America, Medellín, Colombia, September 2014. https://doi.org/10.2118/171105-MS.

Gilman, J.R. and MacMillan, D.J. 1987. Improved Interpretation of the Inaccessible Pore-Volume Phenomenon. *SPE Formation Evaluation* **2**(4): 442-448. doi:10.2118/13499-PA.

Green, D.W., and Willite, G.P. 1998. *Enhanced Oil Recovery.* Textbook Series, SPE, Richardson, Texas **6**: 100–185.

Jouenne, S. and Levache, B. 2020. Universal Viscosifying Behavior of Acrylamide-Based Polymers Used in Enhanced Oil Recovery. *Journal of Rheology* **64**(5) 1295-1313. doi: 10.1122/8.0000063.

Lotsch, T., Muller, T., Pusch, G. 1985. The Effect of Inaccessible Pore Volume on Polymer Core Experiments. Paper SPE 13590 presented at the International Symposium on Oilfield and Geothermal Chemistry. Phoenix, AZ. 9-11 April. doi: 10.2118/13590-MS.

Manichand, R.N., and Seright, R.S. 2014. Field vs Laboratory Polymer Retention Values for a Polymer Flood in the Tambaredjo Field. *SPE Res Eval & Eng*. **17**(3): 314-325 doi: 10.2118/169027-PA.

Seright, R., Maerker, J., and Holzwarth, G.1981. Mechanical Degradation of Polyacrylamides Induced by Flow Through Porous Media. American Chemical Society Polymer Preprints, 22: 30–33.

Seright, R. 1991. Effect of Rheology on Gel Placement. *SPE Res Eng* **6**(2): 212–218; *Transactions AIME* **291**. SPE 18502. doi: 10.2118/18502-PA.

Seright, R.S., Prodanovic, M., and Lindquist, W.B. 2006. X-Ray Computed Microtomography Studies of Fluid Partitioning in Drainage and Imbibition Before and After Gel Placement. *SPE Journal* **11** (2): 159–170. doi: 10.2118/89393-PA.

Seright, R., Lindquist, W., and Cai, R. 2009. Pore-Level Examination of Gel Destruction During Oil Flow. *SPE Journal* **14**(3): 472-476. doi: 10.2118/112976-PA.

Seright, R. 2010. Potential for Polymer Flooding Viscous Oils. *SPE Reservoir Eval. & Eng.* **13**(4): 730–740. doi: 10.2118/129899-PA.

Seright, R.S. 2017. How Much Polymer Should Be Injected during a Polymer Flood? Review of Previous and Current Practices. *SPE Journal* **22**(1): 1-18. doi: 10.2118/179543-PA.

Seright, R.S. Wang, D. 2022. Polymer Retention Tailing Phenomenon Associated with the Milne Point Polymer Flood. *SPE Journal* **27**. doi:10.2118/209354-PA.

Seright, R.S. Wang, D. 2023a. Literature Review and Experimental Observations of the Effects of Salinity, Hardness, Lithology, and ATBS Content on HPAM Polymer Retention for the Milne Point Polymer Flood. *SPE Journal* **28**(05): 2300-2315. doi:10.2118/212946-PA.

Seright. R.S., Wang, D. 2023b. Polymer Flooding: Current Status and Future Directions. *Petroleum Science* **20**(2023): 7 February. doi: 10.1016/j.petsci.2023.02.002.

Seright, R.S., Jouenne, S., Aften, C. 2025. Effect of Salinity and Hardness on HPAM Rheology in Sandstone. *SPE Journal* **30**. doi:10.2118/224231-PA.

Skauge, T., Sorbie, K., Al-Sumaiti, A., Masalmeh, S., Skauge, A. 2021. Polymer in-Situ Rheology in Carbonate Reservoirs. Paper SPE 207286 presented at the Abu Dhabi International Petroleum Exhibition & Conference, Abu Dhabi, UAE, November 2021. doi: 10.2118/207286-MS.

Skoreyko, F., Kumar, A. 2017. Optimized Polymer Injection through Modeling: from Lab to Field. YouTube video: https://www.youtube.com/watch?v=cWqajk7Vlqo.

Song, H., Ghosh, P., Mejia, M., Mohanty, K. 2022. Polymer Transport in Low-Permeability Carbonate Rocks. *SPE Reservoir Eval. &Eng.* **25**. doi:10.2118/206024-PA.

Sorbie, K.S. 1991. *Polymer-Improved Oil Recovery*. Blackie and Son. Glasgow. 50.

Sorbie, K. and Seright, R. 1992. Gel Placement in Heterogeneous Systems with Crossflow. Paper SPE 24192 presented at the 1992 SPE/DOE Symposium on Enhanced Oil Recovery, Tulsa, Oklahoma, April 22–24. doi: 10.2118/24192-MS.

Souayeh, M., Al-Maamari, R.S., Mansour, A., Aoudia, M., and Divers, T. 2022. Injectivity and Potential Wettability Alteration of Low-Salinity Polymer in Carbonates: Role of Salinity, Polymer Molecular Weight and Concentration, and Mineral Dissolution. *SPE Journal* **27(1):** 840–863. doi: 10.2118/208581-PA.

Stavland, A., Jonsbråten, H.C., Lohne, A., Moen, A., Giske, N.H. 2010. Polymer Flooding – Flow Properties in Porous Media Versus Rheological Parameters. Paper SPE 131103 presented at the SPE EUROPEC/EAGE Annual Conference and Exhibition, Barcelona, Spain, June 2010. doi: 10.2118/131103-MS.

Wang, D., Li, C., & Seright, R.S. 2021. Laboratory Evaluation of Polymer Retention in a Heavy Oil Sand for a Polymer Flooding Application on Alaska's North Slope. *SPE Journal* **25**(4) 1842-1856. doi:10.2118/200428-PA.

Zhang, G., and Seright, R.S. 2014. Effect of Concentration on HPAM Retention in Porous Media. *SPE Journal* **19**(3): 373-380. Paper 166256. http://dx.doi.org/10.2118/166256-PA.

SI Metric Conversion Factors

cp x 1.0*	E-03	= Pa·s
ft x 3.048*	E-01	= m
in. x 2.54*	E+00	= cm
mD x 9.869 233	E-04	= μm^2
psi x 6.894 757	E+00	= kPa

* Conversion is exact.

2026 SPE Improved Oil Recovery Conference

SPE 231509-MS

Testing an Improved Method to Determine Inaccessible Pore Volume

R.S. Seright[1]*

[1]Petroleum Recovery Research Center, New Mexico Tech, Socorro, NM, USA
*Corresponding author; randy.seright@nmt.edu

Abstract

Inaccessible pore volume (*IAPV*) is intended to characterize the fraction of aqueous pore space in a porous medium that is not accessible to flowing polymer. Previous *IAPV* literature is contradictory in that no correlation is evident between measured *IAPV* values and rock permeability or porosity or polymer molecular weight or size in solution. Prior work by Gilman and MacMillan (1987) and Wang et al. (2021) demonstrated that much of the previous contradictory reports may result from the inadequacies of methods to measure *IAPV*. In particular, the "double-polymer/tracer bank" method incorporates a water flush between two polymer/tracer banks. The unfavorable mobility ratio as water displaces the second polymer bank causes viscous fingering and overestimation of *IAPV* if insufficient water is flushed. Dean et al. (2022) proposed a potentially improved method to determine *IAPV*, where a low concentration polymer bank is displaced by a more-concentrated, more-viscous polymer bank—so the mobility ratio is always favorable during the displacement. This paper tests this method for determining *IAPV*.

The tests used sandstone cores and bead packs with permeabilities ranging from 113 to 18600 mD, porosities ranging from 0.188 to 0.402, and core lengths ranging from 30.48 to 122-cm. Many tests involved 500-ppm HPAM (with no potassium iodide tracer) displacing 250-ppm HPAM (with a KI tracer). However, three sets of tests made five replicate determinations of *IAPV* using successive polymer banks with HPAM concentrations starting at 62.5 ppm and doubling in stages to 2000 ppm. This procedure tested the reproducibility of the method and whether the *IAPV* measurement depended on HPAM concentration.

With a given data set, multiple methods can be used to assign an *IAPV* value, including (1) the area between polymer and tracer breakout curves, (2) the difference in pore volume (*PV*) throughput (between polymer and tracer) upon attaining an effluent concentration of 50% of the injected concentration, and (3) the difference in *PV* during first breakout of polymer ahead of tracer. Significant differences in calculated *IAPV* values were noted for these different methods.

In general, the method of Dean et al. (2022) provides a substantial improvement over previous methods when measuring *IAPV*. However, caution must be exercised when interpreting the results of these tests with respect to projecting polymer-flood performance. Important uncertainties arise from assessments of *IAPV*—notably, in rock with permeability above 200 mD. These uncertainties arise partly because polymer retention can vary with polymer concentration—violating a key assumption of the method of Dean et al. From this work, it is arguable whether a significant *IAPV* exists in Berea sandstone or bead packs with permeability greater than 200-mD (when using 18-20-million g/mol HPAM).

Introduction

In concept, inaccessible pore volume (*IAPV*) is the fraction of the aqueous-phase pore volume that cannot be accessed by large polymer molecules (Dawson and Lanz 1972). In addition to pores with very small entry points (pore throats), some (Chauveteau 1981; Sorbie 1991; Stavland et al. 2010; Akbari et al. 2019; Skauge et al. 2021; Dean et al. 2022) argued that *IAPV* could also include pore space close to a pore wall, because the radius of a large polymer molecule limits how close the center of mass for the molecule can approach the rock surface. However, Manichand and Seright (2014), Wang et al. (2021), and Seright and Wang (2023a) pointed out major flaws with these "depletion layer" arguments. *IAPV* has been advocated to accelerate polymer transit of a porous medium, while retention (e.g., adsorption onto the rock) retards it (Green and Willhite 1998). Thus, one might argue that *IAPV* facilitates oil displacement, although some have speculated that oil trapped in *IAPV* pores may no longer be available for displacement (Delamaide 2014. Akbari et al. 2019).

The double polymer/tracer method. The above conceptual arguments and definitions may need refinement in view of substantial limitations associated with existing methods of measuring *IAPV*. Although a number of methods have been used in the past (Dawson and Lantz 1972; Manichand and Seright 2014; Akbari et al 2019; Seright and Wang 2023a), the most accepted method to measure *IAPV* in the petroleum literature has been the "double-polymer/tracer-bank" method (Lotsch et al. 1985). Here (**Figure 1**), a bank containing both polymer (e.g., HPAM) and a water tracer (e.g., potassium iodide, KI) is injected into a porous medium that is saturated with water (containing no tracer). The effluent from the core is monitored for concentrations of both the polymer and the tracer until these concentrations stabilize at the injected values. Then, water without tracer is injected to flush the mobile polymer and tracer from the porous medium. Next, a second bank is injected that contains the same concentration of polymer and tracer as in the first bank, and the effluent polymer and tracer concentrations are again monitored until stabilization at the injected values. *IAPV* is then calculated using Eq. 1

$$IAPV = [\Sigma\ [(C_p/C_{po} * \Delta PV) - (C_t/C_{to} * \Delta PV)]] \quad \text{.....(1)}$$

where C_p is effluent polymer concentration, C_{po} is injected polymer concentration, C_t is effluent tracer concentration, C_{to} is injected tracer concentration, PV is the volume in one pore volume, ΔPV is pore-volume increment. In Eq. 1, the only data used is associated with arrival of the polymer and tracer fronts at the core exit for the second polymer/tracer bank. As illustrated in Figure 1, Eq. 1 measures *IAPV* as the area between the polymer and tracer breakout curves associated with the second polymer/tracer bank.

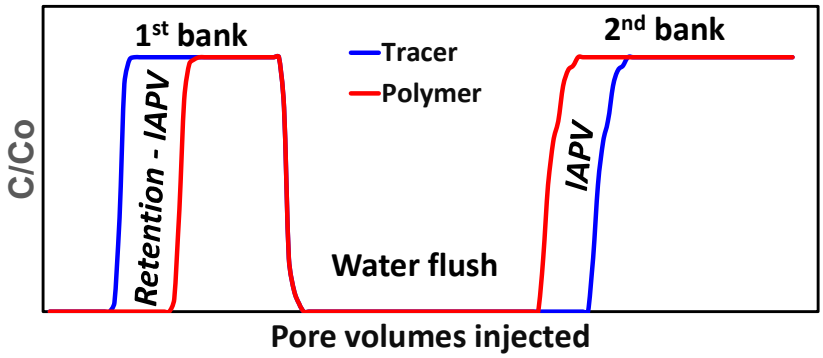

Figure 1—Illustration of the double polymer/tracer bank method to determine *IAPV* and retention.

Polymer retention can then be quantified as the area between the tracer and polymer breakout curves associated with the first polymer/tracer bank, as calculated using Eq. 2.

$$R_{pret} = \{[\Sigma\ [(C_p/C_{po} * \Delta PV) - (C_t/C_{to} * \Delta PV)]] + IAPV\} * C_{po} * PV / M_{rock} \quad \text{.....(2)}$$

where R_{pret} is polymer retention, and M_{rock} is the rock mass in the porous medium.

Inconsistencies from previous measurements. As demonstrated by Manichand and Seright (2014), Wang et al. (2021), and Seright and Wang (2023a), *IAPV* measurements reported in the petroleum literature have been notoriously inconsistent, with no correlation evident between *IAPV* and polymer size, molecular weight, or permeability of the porous medium. Gilman and MacMillan (1987) and Wang et al. (2021) demonstrated that *IAPV* can be substantially overestimated if (1) the tested core is heterogeneous or (2) especially, if insufficient water is flushed through the core between the two polymer banks. When water displaces polymer solution, viscous fingers or channels bypass polymer associated with the first polymer bank of the double polymer/tracer bank method. Unless a very large volume of water is flushed (perhaps 100 *PV* or more), mobile polymer will remain in the core when water injection stops. When the subsequent second polymer is injected, the remaining mobile polymer from the first polymer bank is efficiently displaced to the core outlet—falsely giving the impression that polymer from the second bank is exhibiting *IAPV*. Incidentally, Akbari described a number of variations that have previously advocated to measure *IAPV* (Akbari et al. 2019). All of these methods utilize a water post flush and can be compromised by viscous fingering of water through the polymer bank.

Doubt about interpretation of previously measured *IAPV* values also arises from consideration of the size of polymer molecules in solution, relative to the size of pores and pore throats. For common HPAM polymers used in enhanced oil recovery (e.g., 15-20 million g/mol Mw), molecular size in solution typically ranges from 0.1 to 0.5 μm, depending on salinity (Jouenne and Levache 2020; Seright et al. 2025). X-ray computed microtomography studies (Seright et al. 2006, 2009) demonstrated that over 98% of the pore throats and pore bodies in 470-mD Berea sandstone have effective radii greater than 5 μm (10-50 times the polymer radius). Consequently, virtually all pores in moderated-to-high-permeability (i.e., greater than 500 mD) sand and sandstone should be quite accessible to typical HPAM molecules. Since virtually all large-scale polymer floods comprise of sands and sandstone with permeability larger than 500 mD (Seright and Wang 2023b; Azad and Seright 2025), *IAPV* values less than 2% might be expected in most existing polymer-flooded reservoirs.

Perhaps indicating a lack of confidence in laboratory measurements, some simulators use *IAPV* as an adjustable parameter for history matching (Skoreyko and Kumar 2017). For those cases, it might be more appropriate to call the adjustable parameter a "simulation fudge factor" rather than misleadingly label it as *IAPV*.

The method of Dean et al. (2022). To circumvent viscous fingering associated with water displacing polymer during the double polymer/tracer method (and other previous methods), Dean et al. (2022) advocated injecting a bank with moderate polymer concentration/viscosity, followed by a bank with higher polymer concentration/viscosity **(Figure 2**). Both polymer banks must be large enough so that the effluent concentrations reach the injected concentrations (of polymer and tracer). After normalizing the baselines for the two banks, *IAPV* is established using the second-(high-concentration)-bank polymer breakout curve. The method assumes that polymer retention and *IAPV* are not functions of polymer concentration. The concept has considerable merit in its simplicity and avoidance of viscous-fingering problems associated with other methods for determining *IAPV*. However, additional examination is required because very few reports utilizing the method have been published (Dean et al. 2022), and important details about those tests (e.g., permeability, character of the rock, polymer concentrations) were not disclosed.

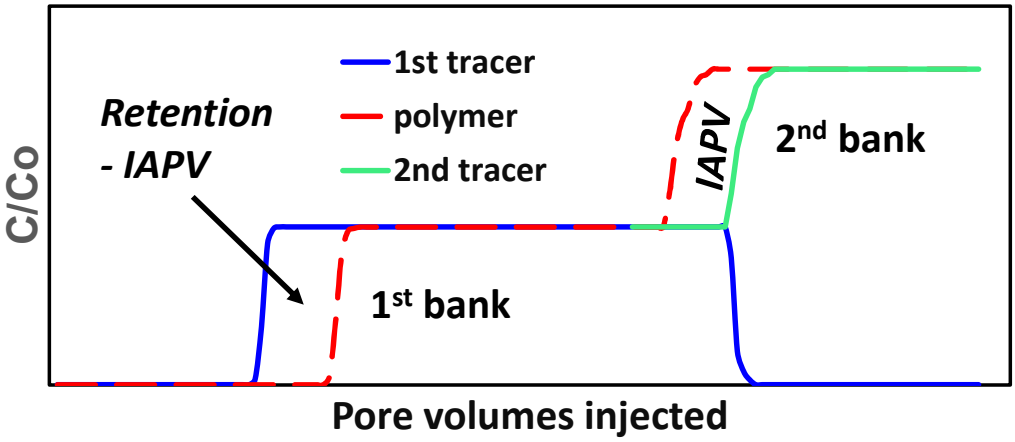

Figure 2—Illustration of method of Dean et al. (2022) to determine *IAPV* and retention.

Consequently, the goal of this paper is to examine the method advocated by Dean et al. (2022). After describing the experimental methodology, polymer retention and *IAPV* values are reported for sandstone cores and bead packs with permeabilities ranging from 113 to 18600 mD, porosities ranging from 0.188 to 0.402, and core lengths ranging from 30.48 to 122-cm (1 to 4 ft). Many tests involved 500-ppm HPAM (with no KI tracer) displacing 250-ppm HPAM (with a KI tracer). However, three sets of tests made five replicate determinations of *IAPV* using successive polymer banks with HPAM concentrations starting at 62.5 ppm and doubling in stages to 2000 ppm. This procedure tested the reproducibility of the method and whether the *IAPV* measurement depended on HPAM concentration. Different methods for assigning an *IAPV* value will be compared, including (1) the area between polymer and tracer breakout curves, (2) the difference in pore volume (*PV*) throughput (between polymer and tracer) upon attaining an effluent concentration of 50% of the injected concentration, and (3) the difference in *PV* during first breakout of polymer ahead of tracer. Finally, the relevance of *IAPV* and the results to field applications will be discussed.

Materials and Methods

Brine, polymer and temperature. The brine used in this work contained 0.2% NaCl. The polymer was Flopaam 3630S™ HPAM, which the manufacturer (SNF) stated had a molecular weight of 18-20 million g/mol and 30% degree of hydrolysis. All experiments were performed at 20°C.

Porous media. The porous media used in this work included Berea sandstone cores and glass bead packs. Permeabilities ranged from 113 mD to 18.6 D, while porosity ranged from 0.188 to 0.402. **Table 1** lists properties of the cores and glass bead packs. Most of the cores and bead packs were 30.48-cm long and 2.54-cm in diameter. However, the 113-mD Berea core was 122-cm long, with a 3.81-

cm x 3.81-cm square cross-section. Most cores and packs were contained in a Hassler cell with 500-psi confining pressure. However, the 113-mD Berea core was cast in epoxy, which limited the pressure and flow rate that could be applied.

Table 1—Summary of porous media and *IAPV* results

Permeability, darcys	Porosity	Core length, cm	Core material	Retention, µg/g	*IAPV*, % *PV*
18.6	0.402	30.48	200-µm glass beads	0.18	0%
17.3	0.377	30.48	200-µm glass beads	0 to 16.6	-5.6 to 2.1%
1.01	0.255	30.48	Berea sandstone	19.8	0%
0.473	0.210	30.48	Berea sandstone	5.43 to 7.4	-1.6 to 4.7%
0.383	0.209	30.48	Berea sandstone	11.9	2.5%
0.209	0.199	30.48	Berea sandstone	0 to 26.3	-36.2 to 26.8%
0.113	0.188	122	Berea sandstone	46	44.6%

Typical flooding procedure. Each porous medium was saturated with 0.2% NaCl brine (without KI tracer) before being flooded with 5-10 *PV* of polymer solution. In most experiments, the Darcy velocity during flooding was 1.86 ft/d. In contrast, the 113-mD Berea core was flooded at 0.89 ft/d to ensure that the pressure across the epoxy-cast core never exceeded 60 psi (which might risk breaching the epoxy). Oil was not used in these experiments. In many experiments, the first polymer bank contained 250-ppm HPAM and 20-ppm KI (and 0.2% NaCl). Also, in many experiments, the first 250-ppm-HPAM polymer bank was immediately followed by a bank containing 500-ppm HPAM (and 0.2% NaCl) with no tracer. With this method, the "tracer" associated with the second, more viscous polymer bank was the absence of the 20-ppm KI. Flow was not stopped when switching from one polymer bank to the next. In particular, the (closed) flow line for the second polymer bank was pressurized to match the pressure of the core inlet pressure at the end of injection of the first polymer bank. Then a three-way valve was opened that switched from injecting 250-ppm HPAM to 500-ppm HPAM. This procedure eliminated pressure surges during the switch.

Flooding procedure with concentration variations. Tables 2, 3 and 4 list the injection sequence during the tests designed to examine how polymer concentration affected *IAPV* determination. For the experiment in Table 2 (in the 17.3-D 200-µm glass bead pack), after brine saturation, the first 5-*PV* polymer solution injected contained 62.5-ppm HPAM, 20-ppm KI and 0.2% NaCl. The second 5-*PV* polymer solution contained 125-ppm HPAM, 0.2% NaCl and no KI. In subsequent tests, the polymer concentration was doubled with each successive polymer bank, and the presence or absence of 20-ppm KI alternated from one bank to the next. Table 3 describes a similar experiment in the 473-mD Berea sandstone core, while Table 4 applies to the 209-mD Berea core.

Effluent analysis. Effluent from packs was analyzed by several methods. A water tracer (20-ppm potassium iodide) was routinely monitored using a Genesys 2™ spectrophotometer at a wavelength of 230 nm. Effluent polymer concentration was monitored by three methods: total organic carbon, total nitrogen, and viscosity. For total organic carbon, a Shimadzu TOC-L™ was used. Total nitrogen was measured using chemiluminescence with a Shimadzu TNM-L™ unit. Viscosity was measured at 7.3 s^{-1} (20°C) using a Vilastic VE™ rheometer. These measurements were made at 4-cm^3 increments for each effluent sample. For figures in this paper, effluent concentrations are reported relative to the injected values. Also, because nitrogen detection is the most reliable measure of HPAM concentration in our case, all effluent polymer concentrations reported in this paper are based on that method.

Table 2—Effect of HPAM concentration on *IAPV* in 17.3-D 200-µm glass beads.

HPAM, ppm	KI, ppm	NaCl, %	Darcy velocity, ft/d	*PV* injected	Viscosity, cp @ 7.3 s^{-1}	Cumulative retention, µg/g	*IAPV*, % *PV*
0	0	0.2	1.86	10	0.9	--	--
62.5	20	0.2	1.86	5	1.3	0.00	--
125	0	0.2	1.86	5	2.6	0.00	2.1
250	20	0.2	1.86	5	5.2	1.13	-3.3
500	0	0.2	1.86	5	11.2	4.6	-5.1
1000	20	0.2	1.86	5	26.5	12.9	-5.6
2000	0	0.2	1.86	5	87.0	16.6	-1.4

Table 3—Effect of HPAM concentration on *IAPV* in a 473-mD Berea core.

HPAM, ppm	KI, ppm	NaCl, %	Darcy velocity, ft/d	*PV* injected	Viscosity, cp @ 7.3 s^{-1}	Cumulative retention, µg/g	*IAPV*, % *PV*
0	0	0.2	1.86	10	0.9	--	--
62.5	20	0.2	1.86	8	1.3	5.43	--
125	0	0.2	1.86	8	2.6	5.43	4.7
250	20	0.2	1.86	7	5.2	5.43	3.7
500	0	0.2	1.86	7	11.2	5.43	1.6
1000	20	0.2	1.86	7	26.5	5.43	4.3
2000	0	0.2	1.86	7	87.0	7.4	-1.6

Table 4—Effect of HPAM concentration on *IAPV* in a 209-mD Berea core.

HPAM, ppm	KI, ppm	NaCl, %	Darcy velocity, ft/d	*PV* injected	Viscosity, cp @ 7.3 s^{-1}	Cumulative retention, μg/g	*IAPV*, % *PV*
0	0	0.2	1.86	10	0.9	--	--
62.5	20	0.2	1.86	8	1.3	0	26.8
125	0	0.2	1.86	8	2.6	0	15.2
250	20	0.2	1.86	7	5.2	0.74	-5.2
500	0	0.2	1.86	7	11.2	11.1	-36.2
1000	20	0.2	1.86	7	26.5	11.1	1.2
2000	0	0.2	1.86	7	87.0	26.3	-13.2

In Tables 2-4, the retention column reports cumulative polymer retention. If the *IAPV* is positive for injection of a given polymer concentration, no additional retention is added to the retention value listed for the previous polymer injection. However, if the *IAPV* value is negative, that value is converted to an additional polymer retention value and added to the retention value listed for the previous polymer injection listing.

Results

Prior to this study, polymer retention and *IAPV* were normally determined using the double polymer tracer method (Lotsch et al. 1985; Wang et al. 2021; Seright and Wang 2022,2023a). By comparing with the current work, determination of *IAPV* using the method of Dean et al. (2022) was found to be far easier and faster to apply reliably than the standard double polymer/tracer method—primarily because it eliminates the need for a very large, time-consuming water bank between injection of the two polymer banks. Also, because the second polymer bank is more viscous than the first, it reduces uncertainty associated with water forming channels or viscous fingers through the first polymer bank.

18.6-D 200-μm glass bead pack. Figure 3 shows effluent tracer and polymer concentrations (relative to injected concentrations) for injection into the 18.6-D pack of 200-μm glass beads (Interactivia #7 grit). (These beads had a very narrow size distribution, as shown in Figure 12 of Seright and Wang 2022). During the first bank of polymer/tracer injection (250-ppm HPAM, 20-ppm KI), the polymer (dashed red curve in Figure 3) and tracer (solid green curve) arrived in the core effluent at the same time and rapidly increased to the injected concentration. After 5 *PV* of 250-ppm HPAM, 5 *PV* of 500-ppm HPAM was injected. Since the 500-ppm HPAM solution contained no KI tracer, the effluent KI concentration dropped to zero after injecting about 1 *PV* (blue curve). For polymer, the previous 250-ppm HPAM concentration was taken is the new "zero" baseline for the second bank, so the dashed black curve in Figure 3 shows the jump in effluent polymer concentration after injecting about 1 *PV* of 500-ppm HPAM. Figure 3 reveals that effluent concentrations stabilized quite quickly after injecting about 1 *PV* of a given polymer/tracer concentration.

Figure 4 replots Figure 3, with a focus on the transitions from one injected polymer concentration to the next. The green and red curves are plotted in the same way as in Figure 3. However, the blue curve from Figure 3 is inverted (going from 0 to 1 instead of from 1 to 0). Thus, for this case, 20-ppm KI was taken as the "zero" baseline, and 0-ppm KI was assigned as full injected concentration of the "tracer". Also, for the blue curve in Figure 4 subtracts 5 *PV* from the throughput in Figure 3, so that the tracer curves from the first and second polymer banks can be compared more closely. This subtraction was also applied to the second-bank polymer data from Figure 3, so that the polymer curves from the two banks can be compared.

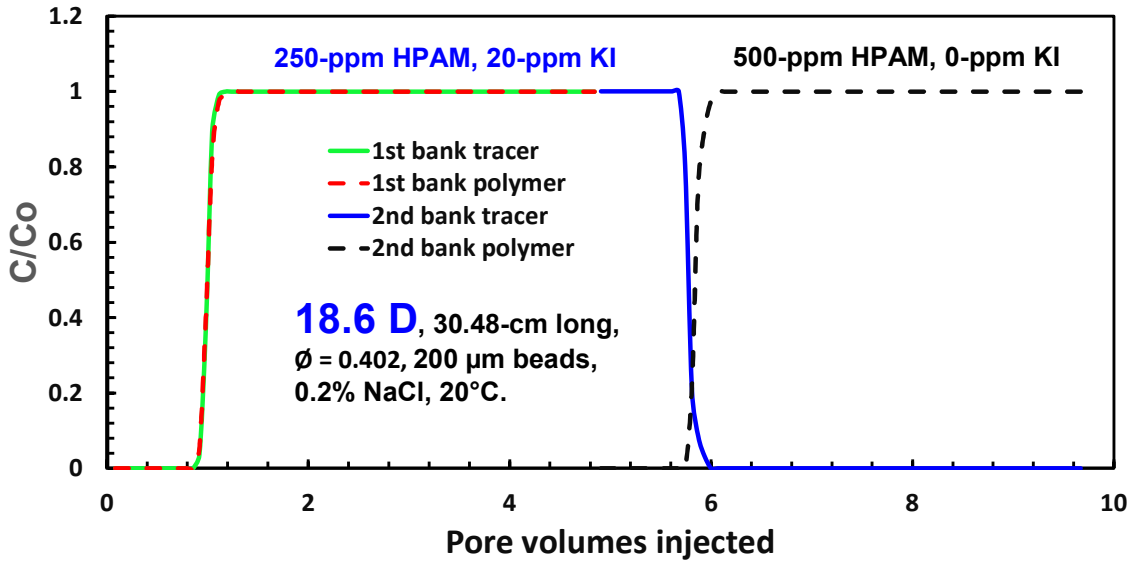

Figure 3—Polymer and tracer effluent concentrations for 18.6-D bead pack.

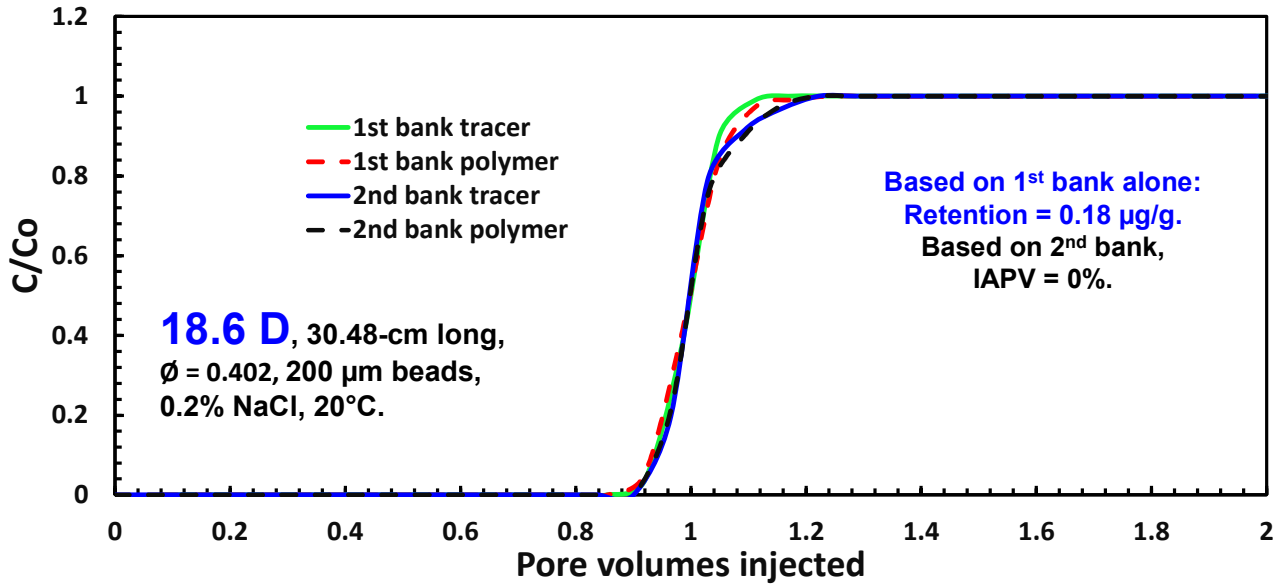

Figure 4—Re-plot of Figure 3, focusing on the transitions.

A comparison of the green and blue curves in Figure 4 reveals that breakout of the KI tracer for the first (250-ppm) polymer bank matched reasonably well with the "tracer" associated with the second (500-ppm) polymer bank. Thus, potassium iodide (and its subsequent displacement) acted as expected as a reproducible water tracer.

If *IAPV* is assumed to be zero, the difference in breakout between the first bank tracer and polymer breakout curves (the green and red curves in Figure 4) provide polymer retention. From Eq. 2, a retention value of 0.18 µg/g was calculated. This very low value is not surprising since the porous medium was 200-µm glass beads.

For polymer breakout during the second bank (500-ppm HPAM), the dashed black curve in Figure 4 matches the other three curves quite closely. As expected, Eq. 1 calculates an *IAPV* value of zero. For closely packed uniform, 200-µm spherical glass beads, pore throats are (mathematically) expected to be in the range from 20 to 40 µm. Consequently, HPAM molecules with ~0.35-µm radius are not expected to experience a significant size-exclusion effect.

Effect of polymer concentration on *IAPV* determination.
The effect of HPAM concentration on *IAPV* determination was investigated. Three sets of experiments were performed—one using 17.3-D 200-µm glass beads; a second using a 473-mD Berea core; and a third using a 209-mD Berea core. As in other cases, the core was first saturated with 0.2% NaCl brine containing no potassium iodide. Next, many pore volumes of polymer solution were injected that contained 62.5-ppm HPAM, 20-ppm KI, and 0.2% NaCl. Effluent tracer and polymer concentration was monitored continuously. Then the sequences indicated in Tables 2, 3 and 4 were followed, injecting polymer banks of increasing concentration. The polymer concentration was doubled with each successive polymer bank, and the presence or absence of 20-ppm KI alternated from one bank to the next. Presumably, polymer retention of the core was satisfied during injection of the first (62.5-ppm HPAM) bank, while replicate *IAPV* determinations could be made during the subsequent five polymer banks.

Tracer consistency. Figures 5, 6 and 7 compare tracer breakout curves associated with the six polymer injection steps of these three experiments. Recall that the tracer is 20-ppm KI for the 62.5-ppm, 250-ppm, and 1000-ppm HPAM cases, while the 125-ppm, 500-ppm, and 2000-ppm HPAM cases used the absence of KI as a tracer. With the minor exception of the 1000-ppm-HPAM case in Figure 6, the various tracer curves overlap quite closely for a given experiment. These results indicate that 20-ppm KI (and its absence) functioned extremely reproducibly as a water tracer. In the 200-µm glass beads (Figure 5), the tracer breakout curves were quite sharp—with first tracer breakout occurring after 0.9 *PV* and full injection concentration reached by 1.1 *PV*. In Berea sandstone, tracer breakout was a bit more disperse—with first tracer breakout occurring after 0.8 *PV* and tracer injected concentration reached about 1.2-1.3 *PV* (Figures 6 and 7).

Polymer breakout curves versus concentration. Figure 8 plots the polymer breakout curves associated with the data in Figure 5 and Table 2; **Figure 9** plots polymer breakout curves associated with the data in Figure 6 and Table 3; while **Figure 10** plots polymer breakout curves associated with the data in Figure 7 and Table 4. Although many pore volumes of polymer solutions were injected during each step, these figures stop at 2 *PV* (or 5 *PV* in the case of Figure 10) to highlight the changes observed. For reference, the blue dashed curve plots a tracer breakout curve. The solid blue curve plots the first breakout of polymer, during injection of 62.5-ppm HPAM.

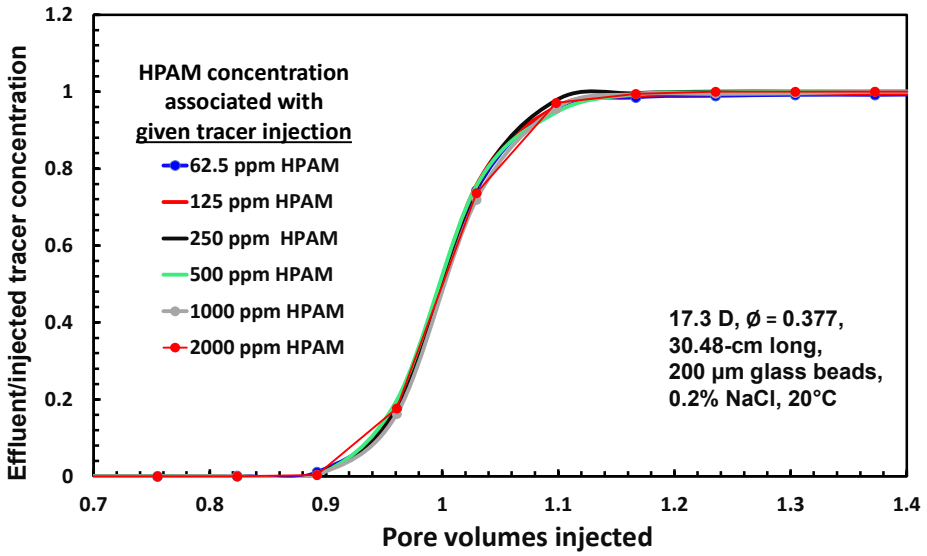

Figure 5—Comparison of tracer breakout curves in the 17.3-D glass bead pack.

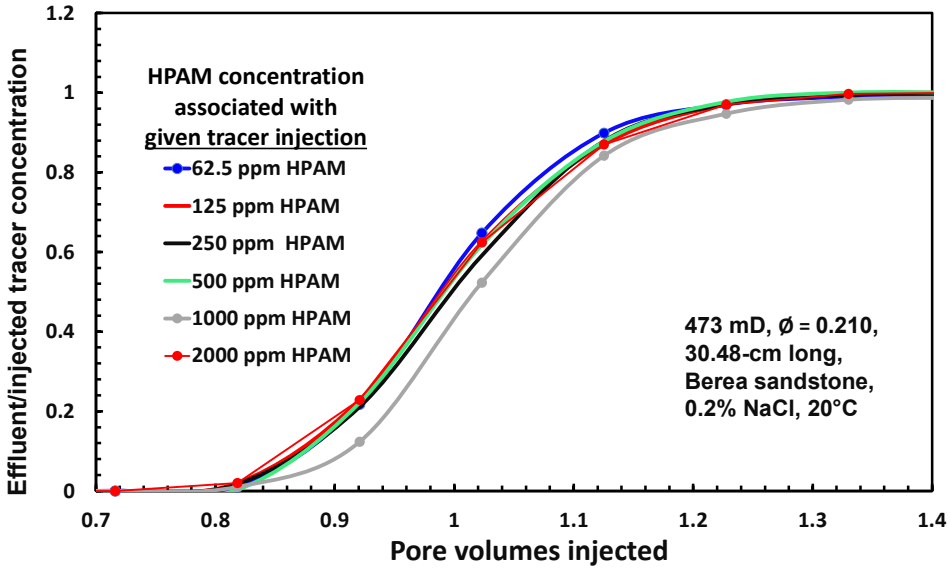

Figure 6—Comparison of tracer breakout curves in the 473-mD core.

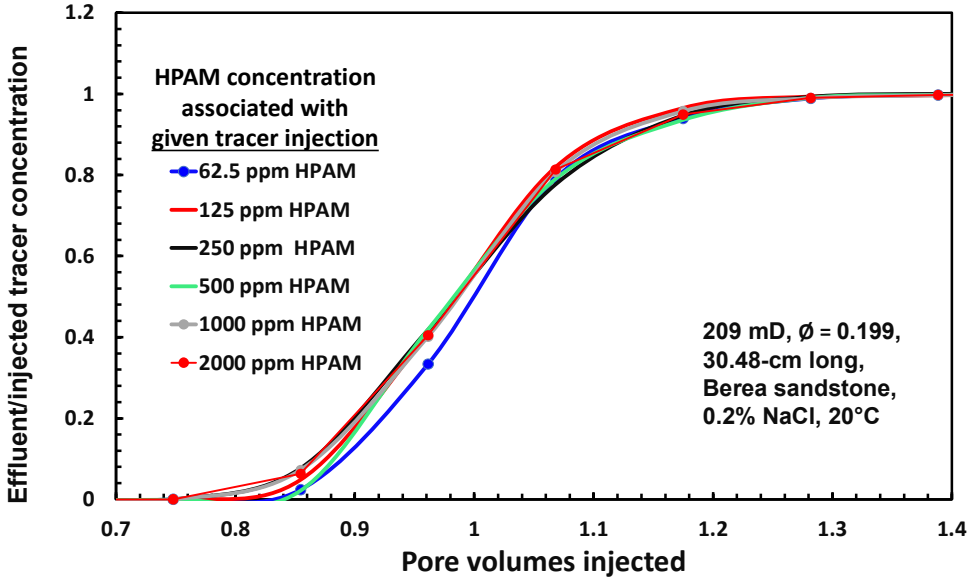

Figure 7—Comparison of tracer breakout curves in the 209-mD core.

17.3-D 200-µm glass bead pack. For Figure 8, using Eq. 2 and the first polymer injected (62.5-ppm HPAM), polymer retention was 0.00 µg/g, which is not surprising since the pack consists of uniform 200-µm glass beads. A close look at the tracer (blue dashed) curve and the 62.5-ppm-HPAM curve reveals that the polymer broke out slightly earlier than the tracer, but the polymer lagged the tracer for a small section in the upper concentrations. The 50%-concentration level was reached at the same time for both tracer and 62.5-ppm HPAM. Thus, the zero-polymer retention resulted from a trade-off from the upper and lower parts of the curves.

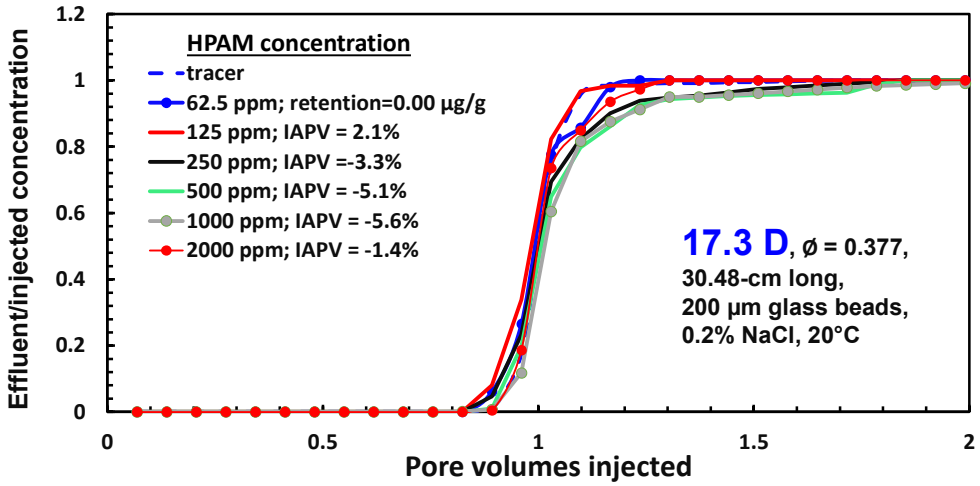

Figure 8—Comparison of polymer breakout curves in the 17.3-D glass bead pack.

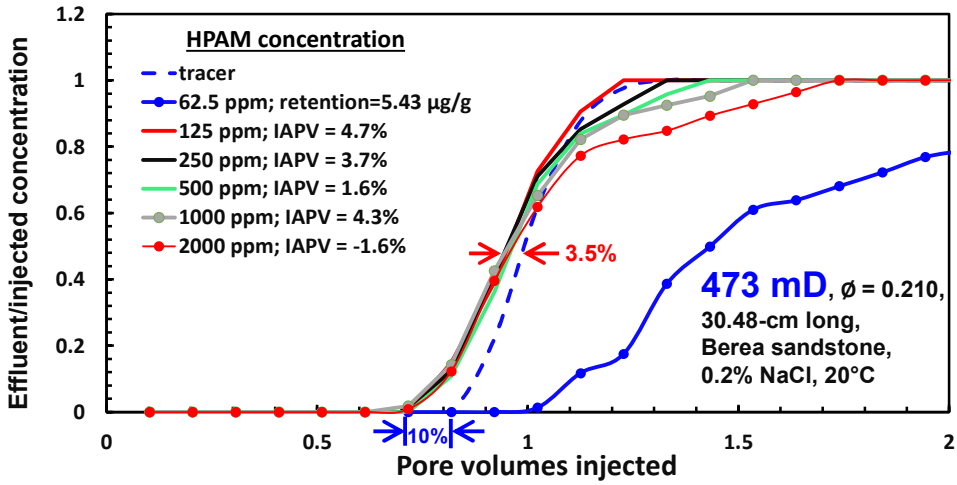

Figure 9—Comparison of polymer breakout curves in the 473-mD core.

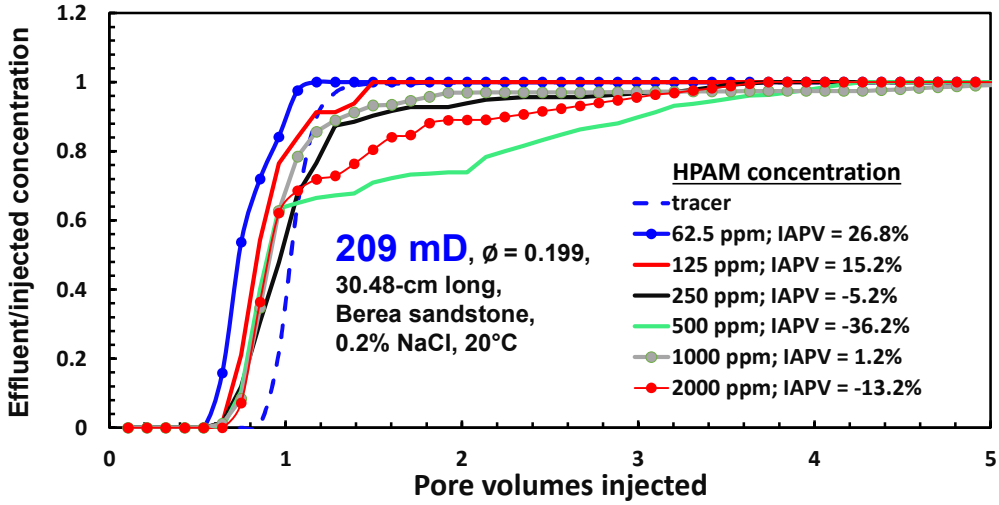

Figure 10—Comparison of polymer breakout curves in the 209-mD core.

In Figure 8 for most concentrations, polymer first arrived in the pack effluent at about the same time as the tracer, although if one wanted to nitpick, it might be said that the 62.5-ppm, 125-ppm, and 250-ppm polymer arrived very slightly ahead (i.e., ~0.85 *PV*) of the tracer and 500-ppm, 1000-ppm and 2000-ppm cases (~0.9 *PV*). The 50%-concentration level was reached at 1 *PV* for the tracer and all polymer cases. Thus, if reaching the 50%-concentration level was the criterion for assessing *IAPV*, one could argue that the *IAPV* was zero for the cases where HPAM concentration was 2000 ppm or less. This is not surprising, since the minimum opening size in these uniform 200-μm glass beads is about 20 μm—compared to ~0.35 μm for a typical 20-million-g/mol HPAM molecule in solution.

Interestingly, if Eq. 1 is formally used to calculate *IAPV*, the *IAPV* values appear to decrease with increased HPAM concentration—from 2.1% to negative 5.6% as polymer concentration increases from 125 ppm to 1000 ppm. A negative *IAPV* value is equivalent to polymer retention being greater during injection of the more-concentrated second polymer bank than during the first polymer bank. If the porous medium exhibits significant retention, the results might be attributed to concentration-dependent adsorption (Zhang and Seright 2014). However, it seems unlikely that any significant adsorption occurs on 200-μm glass beads (see the first two data rows of Table 1). Thus, one might argue that the *IAPV* range from -5.6% to 2.1% simply reflects experimental variation for this case.

473-mD Berea sandstone core. Figure 9 shows polymer breakout curves for the 473-mD Berea core. Assuming *IAPV* =0, Eq. 2 calculates a polymer retention value of only 5.43 μg/g. The solid red curve with no symbols illustrates polymer breakout during injection of 125-ppm HPAM to provide the first measure of *IAPV*. From Eq. 1, the data yielded an *IAPV* of 4.7%. The black, green, grey, and red-dot curves show polymer breakouts during subsequent injection of 250-ppm, 500-ppm, 1000-ppm, and 2000-ppm HPAM—yielding *IAPV* values of 3.7%, 1.6%, 4.3%, and negative 1.6%, respectively.

For all five of the *IAPV* curves in Figure 9 (i.e., 125-ppm to 2000-ppm HPAM), polymer first arrived at the core outlet at 0.7 *PV*—compared to slightly over 0.8 *PV* for the tracer. Also, these five curves closely overlapped and were to the left of the tracer curve up to 0.5 *PV*. Consequently, below 0.5 *PV*, one could argue that *IAPV* accelerated HPAM propagation by about 10% at first polymer breakout, but that effect diminished to about 3.5% by 0.5 *PV*. Beyond 0.5 *PV*, the five curves diverged, with the extent of delay or "tailing" increasing with increased polymer concentration. Thus, in contrast to the behavior before 0.5 *PV*, the polymer generally propagated slower than the tracer after 0.5 *PV*. The 125-ppm-HPAM curve most closely matched the tracer curve. As shown in Figure 9 and Table 3, *IAPV* values can be calculated (using Eq. 1) for these curves—with values ranging from -1.6% to 4.7%. However, it is arguable whether the effects seen are necessarily due to size-exclusion.

A message from Figure 9 might be that *IAPV* assessments made using lower polymer concentrations are more likely to be credible than using higher polymer concentrations.

209-mD Berea sandstone core. Figure 10 shows polymer breakout curves for the 209-mD Berea core. Assuming *IAPV* =0, Eq. 2 calculates a polymer retention value of about *negative* 2 μg/g. Put another way, if retention is assumed to be zero, Eq. 1 projects that the *IAPV* is 26.8%. As indicated in Figure 10, *IAPV* projections for the subsequent polymer banks yield values of 15.2%, negative 5.2%, negative 36.2%, positive 1.2% and negative 13.2% for polymer concentrations of 125 ppm, 250 ppm, 500 ppm, 1000 ppm, and 2000 ppm, respectively. As mentioned earlier, negative *IAPV* values indicate additional polymer retention. With *IAPV* values ranging from negative 36% to positive 26.8%, an *IAPV* assignment of zero might be as appropriate as any other value for this 209-mD core.

From Figure 10, first polymer breakout occurred at 0.54 *PV* when injecting 62.5% HPAM, compared to first tracer breakout at 0.85 *PV*. For the other five polymer banks, first polymer breakout occurred at 0.64 *PV.* Thus, as for the 473-mD case above (Figure 9), first polymer breakout occurred notably earlier than first tracer breakout, and (except for the 62.5-ppm case) first polymer breakout was not dependent on polymer concentration. If *IAPV* was assigned strictly on first polymer breakout, one might argue that *IAPV* in 209-mD Berea was 21% (e.g., 0.85 minus 0.64). This assignment would be double that for the 473-mD Berea core (Figure 9).

In Figure 10, a notable "tailing" phenomenon occurred for many of the polymer banks—where a substantial number of pore volumes must be injected for the effluent to achieve the injected polymer concentration. This "tailing" was drawn out over 5 PV for some polymer concentrations—substantially longer than observed in the 473-mD case (Figure 9). Interestingly, the most prominent tailing in Figure 10 occurred with the 500-ppm case (solid green curve). This observation suggests that polymer retention in Berea is most sensitive to concentration around 500-ppm HPAM. This suggestion is consistent with Figure 7 of Zhang and Seright (2014). Incidentally, "tailing effects" (such as those show here) were extensively investigated previously and attributed to the presence of clays (especially, kaolinite and illite) (Wang et al. 2021; Seright and Wang 2022,2023a).

If *IAPV* was based on achieving a polymer concentration that was 50% of the injected value, *IAPV* would be close to zero for the cases in Figure 8 (17.3-D beads). For Figure 9 (473-mD Berea), the 50%-concentration-level *IAPV* was about 3.5% for all cases. For Figure 10 (209-mD Berea) the 50%-concentration-level *IAPV* was about 15% for the 500-, 1000-, and 2000-ppm cases, but varied from 7% to 25% for the 62.5-, 125- and 250-ppm cases.

For comparison, if *IAPV* was based on the difference between the first polymer arrival and the first tracer arrival, *IAPV* would be close to zero for the cases in Figure 8 (17.3-D beads), about 10% for 473-mD Berea (Figure 9), and about 20% for most of the cases (excluding the 62.5-ppm case) in 209-mD Berea (Figure 10).

Which *IAPV* value should be used? In the vast majority of cases *IAPV* is used as an input parameter during simulations or fractional flow calculations to assess the efficiency with which injected polymer displaces oil. Those calculations are dominated by the polymer properties at the highest polymer concentrations. This realization indicates that the formally accepted method of determining *IAPV* (i.e., Eq. 1) should be applied. (However, we noted that the form of the actual polymer breakout curves may be substantially different from those symmetrical forms assumed during simulations of polymer flooding.) Polymer viscosity at low concentrations (i.e., first polymer breakout or achieving 50% of the injected concentration) do not contribute as significantly to enhancing oil displacement. During polymer flood simulations or fractional flow calculations, the *IAPV* parameter is input in a form such that higher *IAPV* values accelerate the movement of the full-polymer-concentration polymer and the displacement of oil. However, the behavior in the 209-mD core (Figure 10) is clearly not consistent with the *IAPV* form that is assumed as input during simulations or fractional flow calculations, and it is clearly not accelerating the movement of the highest polymer concentrations. Thus, the *IAPV* concept may be inappropriate and largely meaningless from the viewpoint of improving sweep efficiency in rock such as 209-mD Berea sandstone.

One might speculate that concentration-dependent *IAPV* values occur because of increased polymer entanglements and network formation at higher HPAM concentrations—suggesting that entangled polymers effectively make a gel particle that is too large to pass through some pore throats. However, the available evidence (De Gennes 1979; Seright et al. 1981.2025) reveals that these entanglements are too weak for this suggestion to be viable. [Further, if this explanation was valid, first polymer breakout in Figures 9 and 10 should not have been independent of polymer concentration (from 125-2000 ppm).] At any rate, the results suggest caution when assessing *IAPV* using these types of experiments and especially, the current methods of applying the results to prediction of acceleration of polymer and oil banks during a polymer flood.

Could the tailing effect be caused by something other than polymer retention or inaccessible pore volume? In particular, could the behavior be due to polymer rheology coupled with heterogeneity in the porous medium? Consider a two-layer porous medium where free crossflow can occur between two layers. Previous work (Seright 1991; Sorbie and Seright 1992; Seright 2010) demonstrated that if a viscous polymer solution displaces water, any common polymer rheology (i.e., Newtonian, shear-thinning, shear-thickening) will improve displacement efficiency (i.e., make the polymer front travel farther in the less-permeable layer, relative to the more-permeable layer). In contrast, if the two-layered porous medium is completely filled with a shear-thinning fluid (as is the case for the second and subsequent polymer banks in our *IAPV* experiments), the velocity contrast (v_1/v_2) is proportional to the permeability contrast (k_1/k_2) raised to a certain power. If that power is 1.5 (which may be common for somewhat concentrated polymer solutions in enhanced oil recovery, and if the permeability contrast is 10 to one (Seright 2010), the fluid velocity would be 32 times greater in the high-permeability layer than in the less-permeable layer. Thus, one might suspect this effect of providing an apparent acceleration of the more concentrated polymer through the most-permeable pathway. However, one would expect an equivalent acceleration of the tracer—which clearly did not happen in any of the figures in this paper. Also, if there was a significant heterogeneity to the bead pack or core, the effluent tracer concentration should have exhibited a notable tail (as tracer gradually was produced from the less-permeable pathways). The fairly sharp and symmetric tracer breakout curves shown in this paper argue against the existence of any significant heterogeneity.

Figure 11 (after Figure 5 of Sorbie and Seright 1992) illustrates how cross-flow between high- and low-permeability pathways could result in a tailing effect when a more-viscous fluid displaces a less-viscous fluid. Crossflow from Layer 1 into Layer 2 creates the angled red-blue interface in Layer 2. When the polymer front reaches the core outlet, a concentration tailing phenomenon will be observed as more polymer arrives from Layer 2 with increased throughput. However, as with the previous argument, if this scenario was valid, the produced tracer profile should also have exhibited the tailing phenomenon. Again, since all the produced tracer profiles were sharp and exhibited no sign of tailing, the presence of significant heterogeneity seems unlikely.

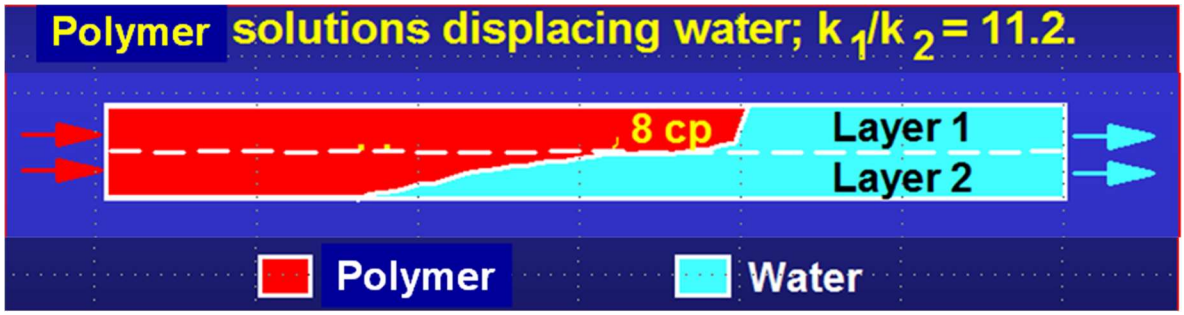

Figure 11—Possible rheology origin of tailing effect. After Figure 5 of Sorbie and Seright 1992.

***IAPV* in sandstones with other permeabilities**

383-mD Berea sandstone core. Figure 12 shows the results of *IAPV* experiments in 383-mD Berea sandstone. In this experiment, seven *PV* of 250-ppm HPAM (with 20-ppm KI tracer) was followed by seven *PV* of 500-ppm HPAM (without KI tracer). The solid blue and green curves demonstrate that the tracer breakout curve during the second polymer bank matched well with the tracer curve

during the first polymer bank. The dashed red curve shows HPAM breakout during the first polymer injection bank, which ultimately (after accounting for 2.5% *IAPV*) yielded a polymer retention value of 11.9 µg/g.

Different ways to calculate *IAPV*. The dashed black curve shows HPAM breakout during the second polymer bank. Similar to the 500-ppm-HPAM case in Figure 9, the polymer first arrived at the core outlet after 0.7 *PV*, which again, was earlier than the first tracer arrival (at ~0.9 *PV*). Thus, if *IAPV* were defined as the difference between first polymer breakout and first tracer breakout, *IAPV* would be about 20%. The second-bank HPAM curve remained to the left of the tracer curve until about 1 *PV*, after which the HPAM curve lagged significantly from the tracer curve. If attaining 50% of the injected concentration was used as the criterion, IAPV would be 9%. In contrast, Eq. 1 calculates an *IAPV* of 2.5%, but it is arguable how much size-exclusion contributes to the behavior observed. In particular, there may be difficulty envisioning that size-exclusion accounts for the lower-than-expected HPAM concentrations (in the second polymer bank) after 1 *PV*. If one only considers the area where the second polymer bank (the black dashed curve in Figure 12) is to the left of the second tracer bank (the solid blue curve), the *IAPV* value would be 10.4%. In that case, the area where polymer concentrations were less than the tracer concentrations (i.e., to the right of and under the blue curve but above the black dashed curve) yields a polymer retention of 3 µg/g associated with the second polymer injection.

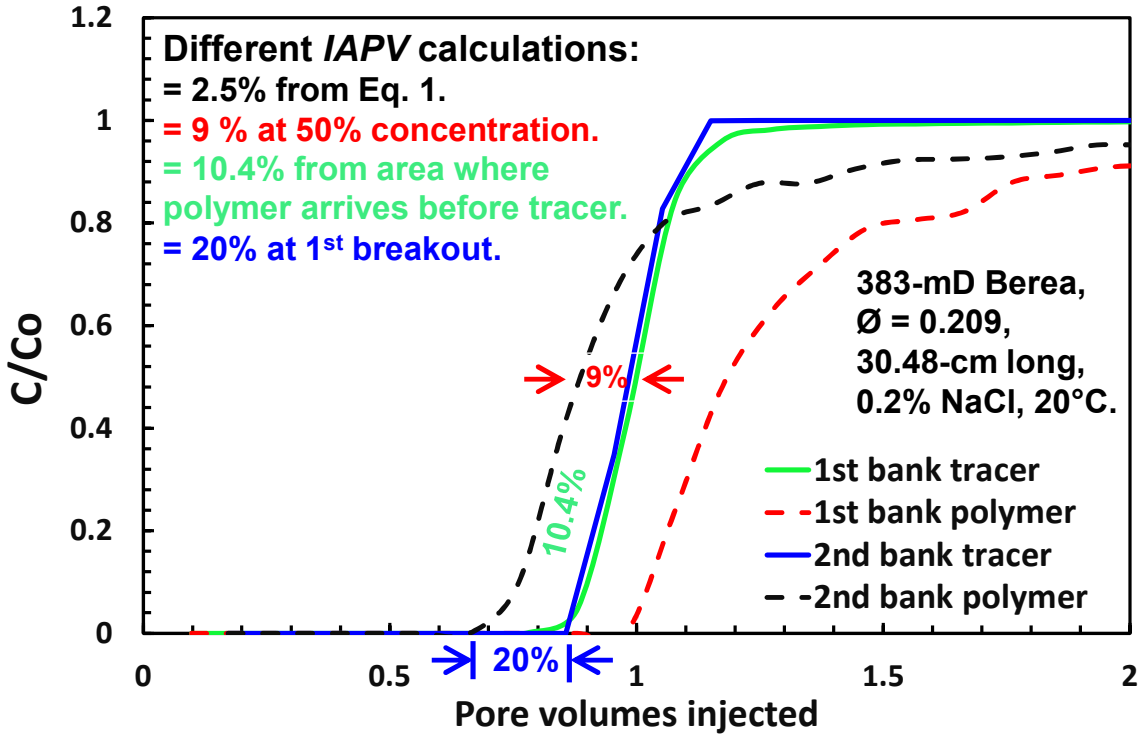

Figure 12—*IAPV* determination in a 383-mD core.

113-mD Berea sandstone core. Figure 13 shows the results of *IAPV* experiments in 113-mD Berea sandstone. In this experiment, 4.2 *PV* of 250-ppm HPAM (with 20-ppm KI tracer) was followed by 5 *PV* of 500-ppm HPAM (without KI tracer). This 122-cm long core had a large pore volume (334 cm^3), which allowed effluent samples to be collected every 1% *PV* (compared to ~10% *PV* for the studies described above). The dashed red curve shows HPAM breakout during the first polymer injection bank, which ultimately (after accounting for 44.6% *IAPV*) yielded a polymer retention value of 46 µg/g. If *IAPV* was assumed to be zero, HPAM retention would have been 24 µg/g. As with all experiments reported in this paper, after tracer breakthrough, no face plugging or gradual rise in pressure was observed during the course of polymer injection. Further, no accumulation of polymer or gel was noted on the inlet or outlet core faces at the end of the experiment.

The dashed black curve shows HPAM breakout during the second polymer bank. Interestingly, for this case, the polymer breakout was definitively ahead of the tracer breakout at all times, and the polymer "tailing" effect seen in Figures 9, 10, and 12 was not evident. The calculated *IAPV* was 44.6% using Eq. 1, 43% based on attaining 50% effluent concentration, and 36% based on first breakout. These values are high but not unreasonable, considering the low-permeability of the core.

Others have understandably asserted that low-permeability rocks may possess a significant fraction of pores that are not accessible by high-Mw polymers, especially carbonates that have a bimodal pore size distribution. For example, Souayeh et al. (2022) reported *IAPV* values up to 68% in 200-300-mD Indiana limestone where 56% of the pores were below 1 µm. Interestingly, Song et al. (2022) observed *IAPV* values from 0-11% in <50-mD Edwards Yellow limestone cores where 90% of the pore throat openings were between 1 and 10 µm.

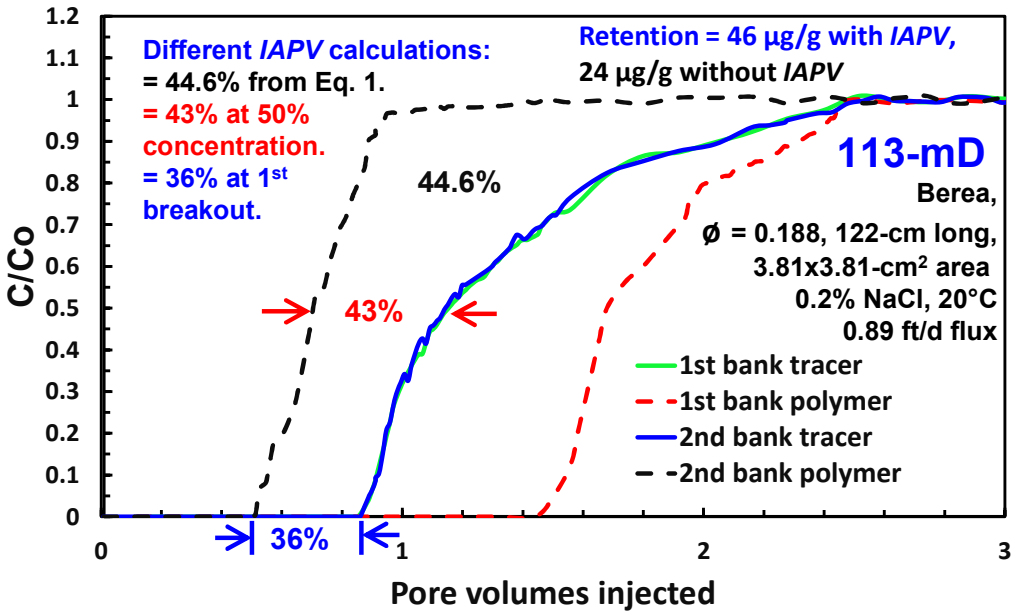

Figure 13—*IAPV* determination in a 113-mD core.

Discussion

Our experience with the method of Dean et al. (2022) reveals that it is substantially easier, faster and more reliable for determining *IAPV* than the double polymer-tracer-bank method (Lotsch et al. 1985). Past analysis (Manichand and Seright 2014; Wang et al. 2022; Seright and Wang 2024) revealed that few people have the patience to inject a sufficiently large brine bank when using the double polymer-tracer-bank method.

That being said, even with the superior method of Dean et al. (2022), substantial uncertainties arise from assessments of *IAPV*—notably, in rock with permeability above 200 mD. As demonstrated during the discussion of Figures 9, 10 and 12, there are multiple methods that could be used to assign an *IAPV* value, including (1) the formally accepted method of Eq. 1, (2) the difference in *PV* (between polymer and tracer) upon attaining an effluent concentration of 50% of the injected concentration, and (3) the difference in *PV* during first breakout of polymer ahead of tracer. The figures in this paper revealed significant differences in calculated *IAPV* values for these methods.

A curious result from Figures 9, 10 and 12 is that during the second (or subsequent) banks of polymer injection, the effluent polymer concentration commonly fell below the tracer concentration (relative to the injected concentrations) during part of the injection process. One interpretation of this result was that polymer retention varied with polymer concentration (in violation of a key assumption in the method of Dean et al. 2022). This interpretation is consistent with reports from Zhang and Seright (2014) for the range of polymer concentrations tested in this work. Nevertheless, in Figures 9, 10 and 12, one wonders why some level of apparent *IAPV* is seen upon first polymer breakout, but polymer retention/retardation is evident later at higher effluent concentrations. Figures 9 and 10 imply that if *IAPV* is based only on first polymer/tracer breakout, the *IAPV* is independent of polymer concentration (from 125 to 2000 ppm). One might rationalize that regardless of polymer concentration, the same fraction (e.g., 10-20%) of the largest polymer molecules travel rapidly through the most-permeable pathway (and presumably the largest pores) where the area for adsorption may be less than in less-permeable pathways. Subsequently, the remainder of polymer molecules displace less-concentrated polymer from the smaller pores, where concentration-dependent adsorption/retention becomes evident.

As mentioned above, the presence of true excluded volume effects is not surprising in low-permeability rock (e.g., less than 200 mD for 18-20-million g/mol HPAM). However, virtually all existing large-scale polymer floods occur in reservoirs where most of the rock/sand is more permeable than 500 mD (Seright and Wang 2023b; Azad and Seright 2025). (And all the existing large-scale polymer floods use HPAM with similar composition and Mw as that in this work.) Thus, it seems reasonable to question the need, the practicality and the value of utilizing the *IAPV* concept for these polymer floods. Of course, the suggested 200-mD limit (for applicability of the *IAPV* concept) applies here to HPAM with 18-20-million g/mol Mw, since that is the only polymer used in this work. Presumably, that limit might be raised for lower-Mw polymers and lowered for higher-Mw polymers.

As pointed out in the Introduction, some simulators use *IAPV* strictly as an adjustable parameter to facilitate their history matching. It would be more honest and functional to not label an adjustable parameter as *IAPV*. If improvements in the operation of the polymer flood are to be identified (e.g., changing the polymer Mw or polymer concentration or bank size), successful alterations are far more likely to result through insights from real physical phenomena, rather than unrealistic fiction.

The *IAPV* concept is primarily used during simulations and/or fractional flow calculations to judge whether and the extent of *IAPV* in accelerating the main body of the polymer bank and any oil bank through a reservoir during a polymer flood (Green and Willhite 1998). The input form of *IAPV* for these simulations/calculations commonly assumes that the polymer concentration will rapidly rise from low values to near-injection concentrations over a short distance around the polymer front (Green and Willhite 1998). These assumptions may not be consistent with the true form of polymer propagation (see Figures 9, 10, and 12 and the figures in Wang et al. 2021; Seright and Wang 2022,2023a)—thus, further compromising the *IAPV* concept for common medium-to-high-permeability applications.

From a practical viewpoint, would the actions mimicked during an *IAPV* laboratory experiment be relevant to a field application? In most polymer flood applications, polymer of a single concentration is injected, and the primary question is how rapidly will the polymer front propagate through the reservoir (and with what concentrations)? During laboratory testing, this question is addressed quite well during the first bank of polymer injection—either with the standard double polymer/tracer bank method or the method of Dean et al. (2022). However, does information collected beyond the first polymer bank provide unambiguous value? Based on this work and previous studies (Seright 2017; Wang et al. 2021), it is not clear that it does. As mentioned above in the section "Which *IAPV* value should be used?", from the viewpoint of reservoir engineering and sweep improvement (with 18-20-million g/mol HPAM in rock with >200-mD permeability), the *IAPV* concept appears inappropriate and largely meaningless in rock that shows the behavior seen in 209-, 383- and 473-mD Berea sandstone (Figures 9, 10 and 12).

Conclusions

1. The method of Dean et al. (2022) is substantially easier, faster and more reliable for determining *IAPV* than the double polymer-tracer-bank method (Lotsch et al. 1985).
2. Nevertheless, important uncertainties arise from assessments of *IAPV.* With a given data set, multiple methods can be used to assign an *IAPV* value, including (1) the area between polymer and tracer breakout curves (Eq. 1), (2) the difference in *PV* (between polymer and tracer) upon attaining an effluent concentration of 50% of the injected concentration, and (3) the difference in PV during first breakout of polymer ahead of tracer. Significant differences in calculated *IAPV* values were noted for these different methods.
3. During the second (or subsequent) banks of polymer injection for several experiments, the effluent polymer concentration commonly fell below the tracer concentration (relative to the injected concentrations) for part of the injection process. One interpretation of this result was that polymer retention varied with polymer concentration (in violation of a key assumption in the method of Dean et al. (2022). In 209-473-mD Berea, this interpretation is consistent with reports from Zhang and Seright (2014) for the range of polymer concentrations tested in this work.
4. From this work, it is arguable whether a significant *IAPV* exists in Berea sandstone or bead packs with permeability greater than 200-mD when using 18-20-million g/mol HPAM.
5. In most polymer flood applications, polymer of a single concentration is injected, and the primary question is how rapidly will the polymer front propagate through the reservoir (and with what concentrations)? During laboratory testing, this question is addressed quite well during the first bank of polymer injection—either with the standard double polymer/tracer bank method or the method of Dean et al. (2022). The value information (to planning of a field project) collected beyond the first polymer bank (during laboratory experiments) is debatable.

Nomenclature

C = effluent concentration, mg/L or ~ppm [μg/g]
C_o = injected concentration, mg/L or ~ppm [μg/g]
C_p = effluent polymer concentration, mg/L or ~ppm [μg/g]
C_{po} = injected polymer concentration, mg/L or ~ppm [μg/g]
C_t = effluent tracer concentration, mg/L or ~ppm [μg/g]
C_{to} = injected tracer concentration, mg/L or ~ppm [μg/g]
HPAM = partially hydrolyzed polyacrylamide or acrylamide-acrylate copolymer
IAPV = inaccessible pore volume
k = permeability, darcies [μm^2]
k_1 = permeability in Layer 1, darcies [μm^2]
k_2 = permeability in Layer 2, darcies [μm^2]
M_{rock} = mass of rock in the sand pack, g
M_w = polymer molecular weight, g/mol [daltons]
PV = pore volumes of fluid injected
ΔPV = pore volumes difference
R_{pret} = polymer retention, μg/g
v_1 = fluid velocity in Layer 1, ft/d [m/s]
v_2 = fluid velocity in Layer 2, ft/d [m/s]
ϕ = porosity

References

Akbari, S. Mahmood, S., Nasr, N., Al-Hajri, S. 2019. A Critical Review of Concept and Methods Related to Accessible Pore Volume during Polymer-Enhanced Oil Recovery. *J. Petroleum Science and Engineering* **182** 106263. doi: 10.1016/jpetrol.2019.106263.

Azad, M., Seright. R.S. 2025. Are Field Polymer EOR Projects Reaping the Benefits of SOR Reduction Due to Polymer Viscoelasticity? *SPE Journal* **30**. doi:10.2118/223155-PA.

Chauveteau, G. 1981. Molecular Interpretation of Several Different Properties of Flow of Coiled Polymer Solutions Through Porous Media in Oil Recovery Conditions." Paper 10060 presented at the SPE Annual Technical Conference and Exhibition, San Antonio, Texas, October 1981. doi: https://doi.org/10.2118/10060-MS.

Dawson, R., and Lantz, R.B. 1972. Inaccessible Pore Volume in Polymer Flooding. *SPE Journal* **12** (5): 448–452. doi: 10.2118/3522-PA.

Dean, R.M., Britton, C.J., Driver, J.W., Pope, G.A. 2022. State-of-the-Art Laboratory Methods for Chemical EOR. Paper SPE 209351 presented at the SPE Improved Oil Recovery Conference, Virtual, April 2022. doi: 10.2118/209351-MS.

De Gennes, P-G. 1979. Scaling Concepts in Polymer Physics. Cornell University Press. Ithaca.

Delamaide, E. 2014. Polymer Flooding of Heavy Oil - From Screening to Full-Field Extension. Paper SPE-171105-MS presented at the SPE Heavy and Extra Heavy Oil Conference: Latin America, Medellín, Colombia, September 2014. https://doi.org/10.2118/171105-MS.

Gilman, J.R. and MacMillan, D.J. 1987. Improved Interpretation of the Inaccessible Pore-Volume Phenomenon. *SPE Formation Evaluation* **2**(4): 442-448. doi:10.2118/13499-PA.

Green, D.W., and Willite, G.P. 1998. *Enhanced Oil Recovery.* Textbook Series, SPE, Richardson, Texas **6**: 100–185.

Jouenne, S. and Levache, B. 2020. Universal Viscosifying Behavior of Acrylamide-Based Polymers Used in Enhanced Oil Recovery. *Journal of Rheology* **64**(5) 1295-1313. doi: 10.1122/8.0000063.

Lotsch, T., Muller, T., Pusch, G. 1985. The Effect of Inaccessible Pore Volume on Polymer Core Experiments. Paper SPE 13590 presented at the International Symposium on Oilfield and Geothermal Chemistry. Phoenix, AZ. 9-11 April. doi: 10.2118/13590-MS.

Manichand, R.N., and Seright, R.S. 2014. Field vs Laboratory Polymer Retention Values for a Polymer Flood in the Tambaredjo Field. *SPE Res Eval & Eng*. **17**(3): 314-325 doi: 10.2118/169027-PA.

Seright, R., Maerker, J., and Holzwarth, G.1981. Mechanical Degradation of Polyacrylamides Induced by Flow Through Porous Media. American Chemical Society Polymer Preprints, 22: 30–33.

Seright, R. 1991. Effect of Rheology on Gel Placement. *SPE Res Eng* **6**(2): 212–218; *Transactions AIME* **291**. SPE 18502. doi: 10.2118/18502-PA.

Seright, R.S., Prodanovic, M., and Lindquist, W.B. 2006. X-Ray Computed Microtomography Studies of Fluid Partitioning in Drainage and Imbibition Before and After Gel Placement. *SPE Journal* **11** (2): 159–170. doi: 10.2118/89393-PA.

Seright, R., Lindquist, W., and Cai, R. 2009. Pore-Level Examination of Gel Destruction During Oil Flow. *SPE Journal* **14**(3): 472-476. doi: 10.2118/112976-PA.

Seright, R. 2010. Potential for Polymer Flooding Viscous Oils. *SPE Reservoir Eval. & Eng.* **13**(4): 730–740. doi: 10.2118/129899-PA.

Seright, R.S. 2017. How Much Polymer Should Be Injected during a Polymer Flood? Review of Previous and Current Practices. *SPE Journal* **22**(1): 1-18. doi: 10.2118/179543-PA.

Seright, R.S. Wang, D. 2022. Polymer Retention Tailing Phenomenon Associated with the Milne Point Polymer Flood. *SPE Journal* **27**. doi:10.2118/209354-PA.

Seright, R.S. Wang, D. 2023a. Literature Review and Experimental Observations of the Effects of Salinity, Hardness, Lithology, and ATBS Content on HPAM Polymer Retention for the Milne Point Polymer Flood. *SPE Journal* **28**(05): 2300-2315. doi:10.2118/212946-PA.

Seright. R.S., Wang, D. 2023b. Polymer Flooding: Current Status and Future Directions. *Petroleum Science* **20**(2023): 7 February. doi: 10.1016/j.petsci.2023.02.002.

Seright, R.S., Jouenne, S., Aften, C. 2025. Effect of Salinity and Hardness on HPAM Rheology in Sandstone. *SPE Journal* **30**. doi:10.2118/224231-PA.

Skauge, T., Sorbie, K., Al-Sumaiti, A., Masalmeh, S., Skauge, A. 2021. Polymer in-Situ Rheology in Carbonate Reservoirs. Paper SPE 207286 presented at the Abu Dhabi International Petroleum Exhibition & Conference, Abu Dhabi, UAE, November 2021. doi: 10.2118/207286-MS.

Skoreyko, F., Kumar, A. 2017. Optimized Polymer Injection through Modeling: from Lab to Field. YouTube video: https://www.youtube.com/watch?v=cWqajk7Vlqo.

Song, H., Ghosh, P., Mejia, M., Mohanty, K. 2022. Polymer Transport in Low-Permeability Carbonate Rocks. *SPE Reservoir Eval. &Eng.* **25**. doi:10.2118/206024-PA.

Sorbie, K.S. 1991. *Polymer-Improved Oil Recovery*. Blackie and Son. Glasgow. 50.

Sorbie, K. and Seright, R. 1992. Gel Placement in Heterogeneous Systems with Crossflow. Paper SPE 24192 presented at the 1992 SPE/DOE Symposium on Enhanced Oil Recovery, Tulsa, Oklahoma, April 22–24. doi: 10.2118/24192-MS.

Souayeh, M., Al-Maamari, R.S., Mansour, A., Aoudia, M., and Divers, T. 2022. Injectivity and Potential Wettability Alteration of Low-Salinity Polymer in Carbonates: Role of Salinity, Polymer Molecular Weight and Concentration, and Mineral Dissolution. *SPE Journal* **27(1):** 840–863. doi: 10.2118/208581-PA.

Stavland, A., Jonsbråten, H.C., Lohne, A., Moen, A., Giske, N.H. 2010. Polymer Flooding – Flow Properties in Porous Media Versus Rheological Parameters. Paper SPE 131103 presented at the SPE EUROPEC/EAGE Annual Conference and Exhibition, Barcelona, Spain, June 2010. doi: 10.2118/131103-MS.

Wang, D., Li, C., & Seright, R.S. 2021. Laboratory Evaluation of Polymer Retention in a Heavy Oil Sand for a Polymer Flooding Application on Alaska's North Slope. *SPE Journal* **25**(4) 1842-1856. doi:10.2118/200428-PA.

Zhang, G., and Seright, R.S. 2014. Effect of Concentration on HPAM Retention in Porous Media. *SPE Journal* **19**(3): 373-380. Paper 166256. http://dx.doi.org/10.2118/166256-PA.

SI Metric Conversion Factors

cp x 1.0*	E-03	= Pa·s
ft x 3.048*	E-01	= m
in. x 2.54*	E+00	= cm
mD x 9.869 233	E-04	= μm^2
psi x 6.894 757	E+00	= kPa

* Conversion is exact.